ARTICLE

Loss-of-Function Mutations in *UNC45A* Cause a Syndrome Associating Cholestasis, Diarrhea, Impaired Hearing, and Bone Fragility

Clothilde Esteve,[1,20] Ludmila Francescatto,[2,20] Perciliz L. Tan,[2,3,20] Aurélie Bourchany,[4,5,21] Cécile De Leusse,[6,21] Evelyne Marinier,[7,21] Arnaud Blanchard,[1] Patrice Bourgeois,[1,9] Céline Brochier-Armanet,[10] Ange-Line Bruel,[4] Arnauld Delarue,[6] Yannis Duffourd,[4,8] Emmanuelle Ecochard-Dugelay,[7] Géraldine Hery,[6] Frédéric Huet,[5] Philippe Gauchez,[6] Emmanuel Gonzales,[11,12] Catherine Guettier-Bouttier,[13] Mina Komuta,[14] Caroline Lacoste,[9] Raphaelle Maudinas,[5] Karin Mazodier,[15] Yves Rimet,[16] Jean-Baptiste Rivière,[4] Bertrand Roquelaure,[6] Sabine Sigaudy,[17] Xavier Stephenne,[18] Christel Thauvin-Robinet,[4,8] Julien Thevenon,[4] Jacques Sarles,[6] Nicolas Levy,[1,9] Catherine Badens,[1,9] Olivier Goulet,[19] Jean-Pierre Hugot,[7] Nicholas Katsanis,[2,3,22] Laurence Faivre,[4,8,22] and Alexandre Fabre[1,6,22,*]

Despite the rapid discovery of genes for rare genetic disorders, we continue to encounter individuals presenting with syndromic manifestations. Here, we have studied four affected people in three families presenting with cholestasis, congenital diarrhea, impaired hearing, and bone fragility. Whole-exome sequencing of all affected individuals and their parents identified biallelic mutations in *Unc-45 Myosin Chaperone A* (*UNC45A*) as a likely driver for this disorder. Subsequent *in vitro* and *in vivo* functional studies of the candidate gene indicated a loss-of-function paradigm, wherein mutations attenuated or abolished protein activity with concomitant defects in gut development and function.

Introduction

The association of congenital diarrhea and hereditary cholestasis in childhood and infancy is rare, and many individuals remain genetically undiagnosed. Recently, some genes identified in one clinical presentation have been expanded to other clinical features. As an example, compound heterozygous and homozygous variants in *myosin VB* (*MYO5B* [MIM: 606540]) have been identified as a cause of congenital diarrhea with microvillus inclusion disease (MVID [MIM: 251850]).[1] Cholestasis, reported as an atypical presentation in MVID, has been considered a side effect of parenteral nutrition. Next-generation sequencing approaches have been necessary to span the clinical spectrum to isolated cholestasis.[2,3] It has been shown that MYO5B, associated with plasma membrane recycling and transcytosis, is essential for polarization of hepatocytes, enterocytes, and respiratory epithelial cells.[4,5] This broadening of clinical spectra has been important for the demonstration that microvilli are markers of disorders in apical-membrane trafficking and assembly, from bowel to liver.[6,7] Such variable clinical presentations have also been demonstrated for other genes responsible for digestive and liver diseases, including *ATP binding cassette subfamily B member 11* (*ABCB11* [MIM: 603201]),[8,9] *tetratricopeptide repeat domain 37* (*TTC37* [MIM: 614589]), and *Ski2 like RNA helicase* (*SKIV2L* [MIM: 600478]).[10–12] Here, we investigated four families presenting with a phenotypic constellation that includes cholestasis, congenital diarrhea, impaired hearing, and bone fragility. We were

[1]Aix Marseille Univ, INSERM, MMG, 13385 Marseille, France; [2]Center for Human Disease Modeling, Duke University, Durham, NC, USA; [3]Department of Cell Biology, Duke University Medical Center, Durham, NC 27701, USA; [4]Equipe GAD, UMR1231 Inserm, Université de Bourgogne Franche Comté, 21079 Dijon, France; [5]Service de Pédiatrie, Hôpital D'Enfants, CHU, 21000 Dijon, France; [6]Service de pédiatrie multidisciplinaire, Hôpital de la Timone Enfants, APHM, 13385 Marseille, France; [7]Service des maladies digestives et respiratoires de l'enfant, Hôpital Robert Debré, APHP, 75019 Paris, France; [8]Centre de Référence Anomalies du Développement et Syndromes Malformatifs et FHU TRANSLAD, CHU, 21000 Dijon, France; [9]Service de biologie moléculaire, Hôpital de la Timone Enfants, APHM, 13385 Marseille, France; [10]Univ Lyon, Université Claude Bernard Lyon 1, CNRS, Laboratoire de Biométrie et Biologie Évolutive (UMR CNRS / Lyon 1 5558), 69622 Villeurbanne, France; [11]Pediatric hepatology and pediatric liver transplantation unit and National Reference Centre for rare pediatric liver diseases, Hepatinov, Bicêtre Universitary Hospital, University of Paris-Sud, Assistance Publique-Hôpitaux de Paris, Le Kremlin Bicêtre, 94800 Villejuif, France; [12]Inserm, UMR-S1174, Hepatinov, University of Paris-Sud 11, 91405 Orsay, France; [13]Pathology Unit, Bicêtre Universitary Hospital, University of Paris-Sud, Assistance Publique-Hôpitaux de Paris, Le Kremlin Bicêtre, 94800 Villejuif, France; [14]Anatomopathology Department, Cliniques Universitaires Saint-Luc, 1200 Brussels, Belgium; [15]Internal medicine and clinical, Hôpital Conception, APHM, 13005 Marseille, France; [16]Service de Pédiatrie-Néonatologie, Centre Hospitalier Intercommunal Aix-Pertuis, 13616 Aix en Provence, France; [17]Département de Génétique Médicale, Hôpital de la Timone Enfants de La Timone, APHM, 13385 Marseille, France; [18]Université catholique de Louvain, Cliniques universitaires St Luc, Département de pédiatrie, Service de gastroentérologie et hépatologie pédiatrique, 1200 Bruxelles, Belgique; [19]Department of Pediatric Gastroenterology, Hepatology and Nutrition, Reference center for Rare Digestive Diseases; Hôpital Necker; University Paris-Cité-Sorbonne; Paris-Descartes Medical School, 75006 Paris, France
[20]These authors contributed equally to this work
[21]These authors contributed equally to this work
[22]These authors contributed equally to this work
*Correspondence: alexandre.fabre@univ-amu.fr
https://doi.org/10.1016/j.ajhg.2018.01.009.

intrigued by the fact that, although several of the presenting features are also encountered in various genetic syndromes, we could not identify examples in the literature in which individuals shared all observed pathologies. Given these observations, we hypothesized that the constellation of phenotypes in the individuals in our study likely represents a clinical entity. To understand the genetic basis of this disorder and to provide an entry point toward both mechanisms and potential therapeutic targets, we studied four individuals from three families. By combining sequencing with functional studies of candidate genes *in vitro* and *in vivo*, we identified Unc-45 Myosin Chaperone A (*UNC45A*) as a driver for this disorder. UNC45A belongs to the UCS protein family (UNC-45/CRO1/She4p) and has not been linked to human genetic disorders. Notably, the *C. elegans* UNC-45 ortholog was first described in a screen for mutations causing motility disorders, a finding likely relevant to the etiopathology seen in humans.

Material and Methods

Whole-Exome Sequencing (WES)

We obtained written consent from parents under a protocol approved by each of our perspective institutional review boards. Genomic DNA was extracted from peripheral-blood samples from the proband and both parents via standard procedures using the Gentra Puregene blood kit (QIAGEN). Family A samples were processed in Dijon University Hospital. The Biobank of the Department of Genetics of La Timone Hospital proceeded with the DNA extraction and ensured the long-term storage of samples from families B and C.

For all individuals (A.II.2, B.II.3, B.II.4, C.II.1, and their parents), whole-exome capture and sequencing were performed at Integragen platform (Integragen SA) from 1.5 μg of genomic DNA per individual using SureSelect Human All Exon V5 kit (Agilent). The resulting libraries were sequenced on a HiSeq 2000 (Illumina) according to the manufacturer's recommendations for paired-end 75 bp reads. Reads were aligned to the human genome reference sequence (GRCh37/hg19 build of UCSC Genome Browser) with the Burrows-Wheeler Aligner (BWA, v.0.7.6a), and potential duplicate paired-end reads were marked with Picard v.1.109. The Genome Analysis Toolkit (GATK) v.3.3-0 was used for base quality score recalibration, indel realignment, and variant discovery (both single-nucleotide variants and indels). Read mapping and variant calling were used for data analysis and interpretation. Variants were annotated with SeattleSeq SNP Annotation 138. Variants present at a frequency >1% in dbSNP 138 and the NHLBI GO Exome Sequencing Project or present from local exomes of unaffected individuals were excluded (see Web Resources). For the individual A, variants were filtered as described.[13] For individuals B.II.3, B.II.4, and C.II.1, variants were filtered with the in-house Variant Analysis and filtration Tool software (VarAFT). Variant filtering followed the following criteria: variants affecting the coding sequence, including (1) splicing and (2) rare variants (<1% allele frequency) from public databases (see Web Resources), (3) homozygous, compound heterozygous, or *de novo* variants. The candidate variants in *UNC45A* were confirmed by Sanger sequencing on a 3500XL Genetic Analyzer (ThermoFisher).

Western Blotting

Fibroblasts of B.II.3 and all the individuals' lymphoblastoid cells (A.II.2, B.II.3, B.II.4, and C.II.1) were lysed by NP40 cell lysis buffer (ThermoScientific) complemented with Halt Proteases and Phosphatases Inhibitor Cocktail 100X (ThermoScientific). After incubation on ice for 30 min, lysed cells were sonicated (4 cycles 15 s on/15 s off), then centrifuged at 16,000 × *g* for 10 min at 4°C. The supernatant was collected and analyzed for protein concentration by Pierce BCA Protein Assay (ThermoScientific). Whole lysates of fibroblasts and lymphoid cells (40 μg per lane) were loaded onto a SDS-PAGE 10% Bis-Tris gel (Bio-rad) for electrophoresis and transferred to a PVDF membrane. The membranes were hybridized with monoclonal mouse anti-human UNC45A antibody (1/1,000; ADI-SRA-1800, Enzo Life Sciences) and with Rabbit anti-human Glyceraldehyde-3-phosphate dehydrogenase polyclonal Antibody (1/10,000) (as loading control; Flarebio Biotech).

In vivo Zebrafish Assays

All animal work was performed with approved protocols from Duke's Institutional Animal Care and Use Committee. To determine the effect of *unc45a* suppression in zebrafish, we designed a splice blocking morpholino (MO) against exon 3 of the zebrafish *unc45a* (ENSDART00000159409.1). To assess efficiency of the MO, we extracted total RNA from control and MO-injected embryos and performed RT-PCR across the site targeted by the MO, followed by sequencing of the RT-PCR products. For the rescue experiments, we *in vitro* transcribed human WT and V423N-encoding mRNA using the SP6 mMessage mMachine kit (Ambion). All injections were done at the 1- to 4-cell stage and each experiment was performed in triplicate as described.[14]

Fluorescent microsphere gavage was performed on 5 dpf zebrafish anesthetized in tricaine and mounted in 3% methylcellulose. Injection of Fluoresbrite polychromatic red 2.0 micron microspheres (Polysciences #19508) was gavaged into the zebrafish intestinal lumen as described.[15] Brightfield and gavage images were taken of 5 dpf embryos using the Nikon AZ100 microscope with a 2× objective and a 5.0-megapixel DS-Fi1 digital camera as previously described.[16]

Serial sections of the zebrafish were obtained by mounting in 3% low-melting point agarose and sections on a vibratome. Standard immunohistochemistry was performed using Phalloidin and 4e8 (both used at 1:1,000 dilution). Sections were mounted onto a coverslip using vectashield and imaged on a Nikon Eclipse 90i with a C2-SH camera at 20×. Image analyses and statistics were performed as previously described.[17]

Results

Clinical Report

All four probands share multiple clinical symptoms including congenital cholestasis, diarrhea, bone fragility with recurrent fractures, and deafness (Figure 1; see detailed clinical report in Supplemental Note). They were assembled together after the discovery of independent homozygous or compound heterozygous variants of *UNC45A*, following a genotype-first approach.

Family A

The proband is a 5-year-old girl of European descent, the second child of unrelated parents with no family history

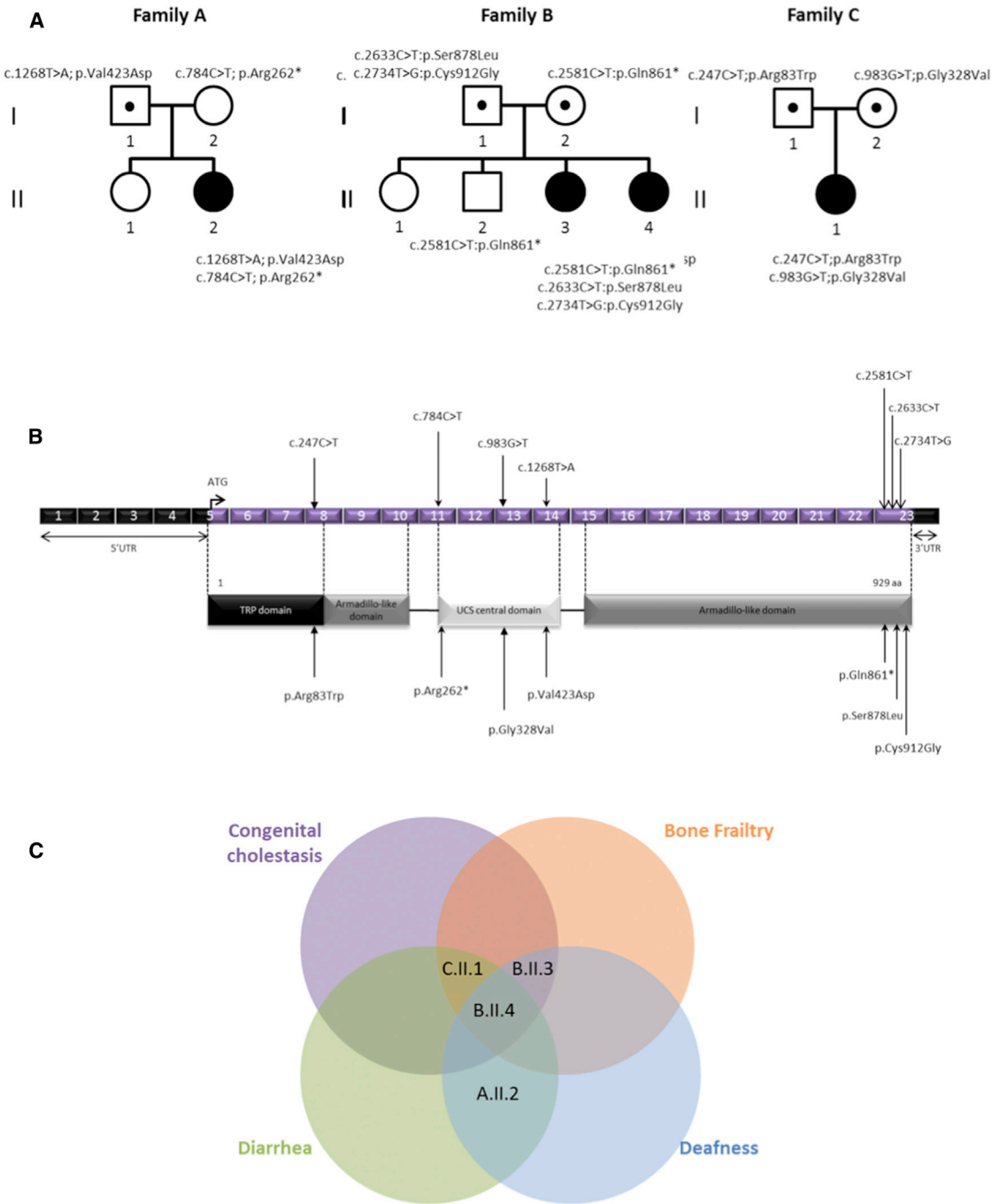

Figure 1. UNC45A Variants and Gene Structure
(A) Pedigrees of the three families with mutations in UNC45A.
(B) Structural organization of UNC45A transcript (Ensembl: ENST00000394275) and protein with known conserved protein domains and localization of amino acid residues affected by mutations identified in the three families. Exonic (in purple) regions are not drawn to scale.
(C) Venn diagram showing the overlap between clinical signs of the four individuals.

of digestive disease. She presented intractable diarrhea requiring parenteral nutrition since her fourth day of life. Her evolution was marked by language delay partially linked to severe bilateral perception deafness; she still has parenteral nutrition. To date, there is no sign of bone fragility or of liver disease.

Family B

Two probands are siblings from unrelated parents, originating from Tunisia. There was no known family history of the clinical presentation observed in the two probands. They have one sister and one brother, both of whom are healthy and have normal height. CGH array did not detect

any chromosome rearrangements and targeted sequencing of known disease genes did not reveal any candidate pathogenic variants.

Individual B.II.3, currently 23 years old, presented at 15 days of life with icteric cholestasis with normal GGT level. Icterus disappeared at 2.5 years but elevated levels of bile acid associated with intractable pruritus remained, leading to partial internal biliary diversion at the age of 19 allowing an amelioration of the pruritus. She presented bone fragility: 23 fractures with normal levels of PTH and vitamin D. Severe bilateral perception deafness was diagnosed in her fifth year. She presented a failure to thrive with a current weight of 38.5 kg and height of 147.5 cm and a slight intellectual disability. (See full report in Supplemental Note.)

Individual B.II.4, currently 18 years old, presented an icteric cholestasis with elevated GGT at 7 days of life. Like her sister, icterus resolved at 3 years, but cholestasis with elevated level of GGT remained as well as elevated levels of bile acid associated with intractable pruritus. These issues led to partial internal biliary diversion at the age of 12, allowing an amelioration of the pruritus. She had bone fragility with multiple fractures and osteonecrosis of the femoral head at the age of 14, secondary to left hip dysplasia at birth and normal calcium phosphate, D vitamin, and PTH levels. Perception deafness was discovered in her teens. Initially, she presented diarrhea requiring parenteral and enteral nutrition. Diarrhea resolved with time, but a failure to thrive persisted at the last evaluation with a weight of 38.5 kg (−3 SD) and a height of 147.5 cm (−2.5 SD) and a mild intellectual disability was noted like her sister.

Family C

The proband is a 5-year-old female born to unrelated parents of Turkish origin. After 15 days of life, the proband presented with cholestatic icterus with normal level of GGT associated with liver failure; both resolved at 4 months of life. She presented bone fragility with two spontaneous fractures, with normal calcium phosphate, PTH, and D vitamin levels. She had diarrhea since the age of 2 months, requiring parenteral nutrition. She continues to have parenteral nutrition and has had recurrent episodes of cytolysis.

Whole-Exome Sequencing of Family A and B Identified Variants in UNC45A

We adopted a genetic approach for the study of a case of intractable diarrhea. The simplex case subject in family A was found in a large cohort of individuals without genetics diagnosis. This study was part of an "undiagnosed program" focusing on the identification of the genetic basis of pathologies in more than 500 affected individuals.

The exome sequencing of this family was first analyzed following a trio strategy. The autosomal-dominant *de novo* hypothesis first allowed the identification of a *de novo* variant in *UNC45A*: c.784C>T (p.Arg262*) encoding a nonsense allele (the RefSeq accession number GenBank: NM_001039675.1 and the transcript ID Ensembl: ENST00000394275.6 was used to name the UNC45A mutations).

A second analysis under the autosomal-recessive hypothesis identified nine genes with homozygous or compound heterozygous variants in their coding region.*UNC45A* and *CLRN2* (*clarin 2*) were considered the strongest candidates: neither has been associated to date with a clinical phenotype in human disease. Among the remaining genes, two have been associated with a human pathology: *FRAS1* (MIM: 607830; phenotype MIM: 136680) and *MYO15A* (MIM: 602666; phenotype MIM: 600316). Frasier syndrome (MIM: 136680) can be likely excluded due to the divergent clinical presentation, while *MYO15A* formally remains a candidate for the deafness phenotype of the individual. However, there are no functional clues about the variant in *MYO15A*, which is thus classified as a variant of unknown significance (VUS). Sanger sequencing for the discovered *UNC45A* mutations confirmed that the missense variant c.1268T>A (p.Val423Asp) was inherited from the father and the stop-gained mutation was *de novo* (compound heterozygous status).

Independently, we performed whole-exome sequencing on genomic DNA from individual B.II.3 and B.II.4 and their parents B.I.1 and B.I.2 (family B; Figure 1). The trio-based analysis did not identify likely clinically relevant variants in known disease-associated genes. Under the hypothesis of either an autosomal-recessive or *de novo* dominant mode of transmission, a search for homozygous, compound heterozygous, or *de novo* rare variants (<0.1% in ExAC Browser and GnomAD) allowed us to identify a unique mutated gene shared by the two sisters: *UNC45A*, a locus not yet associated with any known human genetic disorder. Our exome findings and the high predicted expression levels of *UNC45A* in bone, colon, and liver (Proteomics DB) rendered this locus a strong candidate. The three identified *UNC45A* variants were confirmed by Sanger sequencing and their segregation was consistent with an autosomal-recessive trait (Figure 1). The two missense c.2633C>T (p.Ser878Leu) and c.2734 (p.Cys912Gly) mutations and the nonsense c.2584C>T (p.Gln861*) mutation are all predicted to be damaging by UMD Predictor.[18,19] They are not found in gnomAD database, except for the variant c.2633C>T (p.Ser878Leu) which is reported seven times in the heterozygous state (7/277,162).

Biallelic *UNC45A* variants were the only sites shared among the two unrelated families with overlapping phenotypic features, thereby bolstering our interest for a likely causal association of *UNC45A* variants with the disease presentation.

Additional Families with Phenotypic Match: Discovery of Family C

We added *UNC45A* to our candidate gene list and we reanalyzed the exomes of families without molecular diagnosis

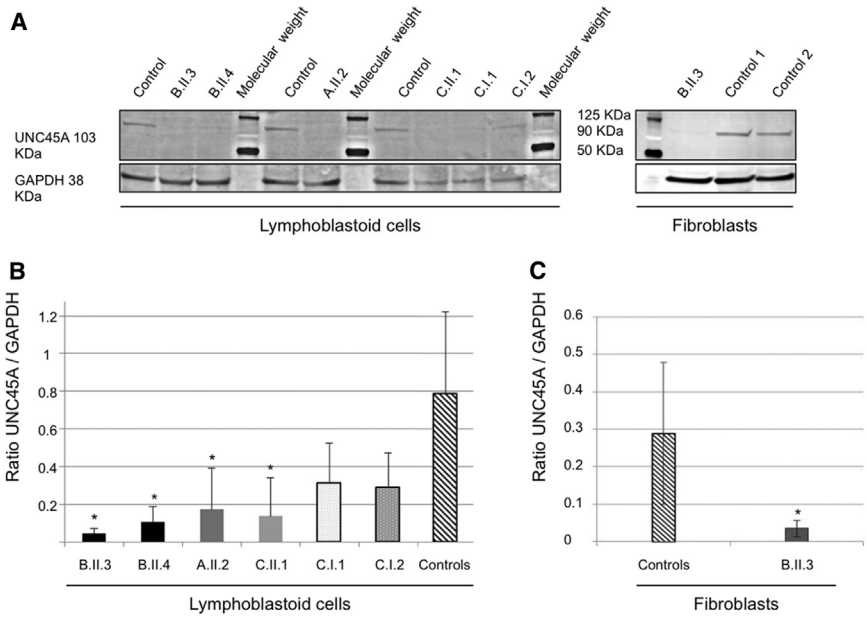

Figure 2. Western Blot Detection and Quantification of UNC45A Protein in Lymphoblastoid Cells and Fibroblasts

(A) Detection of UNC45A by western blot analysis in lymphoblastoid cells and fibroblasts using a monoclonal antibody. GAPDH was used as a loading control.

(B and C) Quantification of UNC45A protein levels with Fiji software shows significantly lowered levels of the expression of UNC45A in all individuals' lymphoblastoid cells (B) and fibroblasts of individual A.II.3 (C). Values are mean ratio ± SD, n = 3; Welch's two sample t test (affected individual versus control) (*$p < 0.04$).

with phenotypes similar to those exhibited by individuals of families A and B. We identified two missense mutations in a third unrelated family presenting liver disease and bone fragility. Specifically, in family C, we identified two missense mutations—c. 247C>T (p.Arg83Trp) and c.983G>T (p.Gly328Val)—in *UNC45A* (Figure 1). These substitutions are predicted to be damaging; one is found only four times (frequency of 4/276,948) in heterozygotes, whereas the second one has never been reported in gnomAD Browser. Given the overlap of clinical features of individual C.II.1 with the clinical spectrum of the other individuals described here, these results provided further evidence for a causal association of biallelic *UNC45A* mutations with this phenotypic presentation.

Functional Impact of Variants Found in UNC45A on Protein Level

To investigate whether these alleles have an effect on protein abundance, we performed western blot using a monoclonal antibody against UNC45A in all the lymphoblastoid cell lines available in our cohort. We detected UNC45A at the predicted size of 103 kDa; quantification of the observed signal in each individual (and the parents of the individual C.II.1) showed a decrease of UNC45A abundance across all individuals' lymphoblastoid cells. Specifically, a significant decrease of protein abundance in each of A.II.2, B.II.3, B.II.4, and C.II.1 (80%, 93%, 89%, and 70% decrease, respectively) compared to control cells (Figures 2C and 2D). Furthermore, we did not detect any signal at ~95 kDa, which would have corresponded to the truncated protein translated from the *UNC45A* allele carrying the nonsense mutation p.Gln861*. The protein absence cannot be explained by NMD since the stop mutation occurs in the last exon of the gene but rather suggests the instability of the truncated protein.

Regarding nonsense variant p.Arg262* in individual A, which maps to exon 11, we likewise did not detect any truncated protein (predicted size ~30 kDa). In this case, due to the position of the stop mutation, NMD could explain this absence. However, the epitope recognized by the antibody remains unknown and could target the deleted part of the protein. Therefore, we cannot formally exclude the possibility of the existence of a truncated protein lacking its C-term part which is known to be critical for nonmuscle myosin II (NM-II) folding.[20] Of note, in family C, the father C.I.1 (who is heterozygous for p.Arg83Trp) and the mother C.I.2 (who is heterozygous for p.Val423Asp) also had reduced UNC45A levels (45% and 52%, respectively), indicating that these alleles are also associated with reduced protein level and lead to the abrogation of protein stability. Together, all these studies suggest a loss of protein abundance/activity paradigm and thus a loss-of-function disorder.

We next asked whether the reduction of UNC45A levels was restricted to lymphoblastoid cells. Using whole-cell lysates from individual B.II.3 fibroblasts, we observed an 82% decrease of UNC45A compared to control cells (Figures 2A and 2C). Similar to the previous experiment, we could not detect any signal that might represent the truncated protein, again suggesting NMD. Quantification of the *UNC45A* mRNA produced in these cells was consistent with this notion; we observed a 40% and 50% decrease of transcripts levels in lymphoblastoid cells of individuals B.II.3 and B.II.4, respectively (Figure S3).

In Vivo Functional Testing of the UNC45A Variation in Zebrafish

With the identification of *UNC45A* likely loss-of-function mutations in affected individuals, we next sought to ask whether dysfunction of this gene contributes to experimentally tractable aspects of the phenotype. We have shown previously the utility of the zebrafish system to assess the involvement of genetic lesions in the formation and function of the gut.[14,21,22] The zebrafish locus is predicted to encode three splice isoforms of *unc45a*; we

focused our studies on the canonical (longest) isoform (ENSDART00000159409.1), which is 64% identical to human UNC45A (ENSG00000140553); the other two isoforms are shorter (230 aa and 218 aa versus 935 aa for the canonical isoform) (Figures S8 and S9). We designed a MO against the splice donor site of zebrafish *unc45a* exon 3. This resulted in the inclusion of intron 3, leading to a premature stop.

To assess one of the primary clinical phenotypes of the affected individuals, congenital diarrhea, we tested the effects of suppression of *unc45a* on both enteric neurons and intestinal motility. We first asked whether this phenotype could be caused by a neurodevelopmental enteric defect. We therefore visualized and counted the neurons along the zebrafish gut by staining with antibodies against HuC/D. In triplicate experiments performed blind to injection cocktail, we could not detect any appreciable difference in the number of enteric neurons in morphants versus controls, suggesting that *unc45a* suppression does not impact neurodevelopment in the gut (Figure S10). Next, we assayed intestinal motility by fluorescent microsphere gavage into the anterior intestine of 5 dpf (days post fertilization) embryos,[15,16] followed by recording of the rate of intestinal motility of the microspheres as a function of time (imaging at 0, 3, 6, 9, and 24 hr). At each time point, we scored in which intestinal zone (1–4, based on anatomical landmarks) the fluorescent microspheres were located as a measurement of transit through the intestine post-gavage. Performing ordinal logistic regression and repeated-measures analysis, we saw that, as time progresses, control larvae are less likely to have microspheres remaining in their intestinal lumen compared to morphants ($p < 0.0001$; OR = 0.504), with a majority of morphants having microspheres remaining in their intestine at 24 hr after gavage. These data suggest that suppression of *unc45a* leads to an intestinal motility defect (Figure 3).

To test this observation further, we turned our attention to a stable genetic model. We obtained the kurzschlusstr12 (kus^{tr12}) zebrafish mutant, an aortic arch mutant identified previously in a forward genetic screen caused by a nonsense mutation in *unc45a*.[23] Although gut motility phenotypes had not been reported previously, such phenotypes are not readily observable; we therefore tested mutants directly by gavage of fluorescent pellets, followed by measurement of the clearance efficiency of these along the alimentary canal as a function of time. Specifically, we divided the gut into four anatomically defined zones and we measured the proportion of embryos that had GFP present in each zone. Consistent with the intestinal phenotype observed in most of our probands, kus^{tr12} mutants had a significant delay in clearing fluorescence that was even more pronounced than what we observed in our morphants. Repeated-measures analysis showed that as time progresses, control larvae are less likely to have microspheres in their intestinal lumen (the majority had no microspheres in their intestines) compared to kus^{tr12} fish ($p = 0.0009$; OR = 0.1387) with the majority of the microspheres in the kus^{tr12} larvae remaining in zone 2 (compared to morphants that showed accumulations primarily in zones 3 and 4 (Figure 3). The observed motility defect was not due to dysfunctional peristalsis, as there was no appreciable peristalsis defect in kus^{tr12} mutants.

We next asked whether the intestinal motility defect could be linked to structural defects. Analysis of peristaltic movement did not show any appreciable differences between WT and mutant larvae (Movie S1), suggesting that a gross defect of the musculature is unlikely. However, observations of control and mutant animals under brightfield showed a lack of folds in the intestine of kus^{tr12} fish. We therefore performed serial sections and used markers for F-actin (Phalloidin) and intestinal brush borders (4e8) to determine whether the defects in intestinal motility we observe in the mutant larvae were the result of structural abnormalities. Analysis of kus^{tr12} mutant and control serial sections revealed defects in the structure of zones 2 and 3 of kus^{tr12} animals (Figure 4). Staining with Phalloidin revealed that, as opposed to having the expected epithelial folds lining the lumen, kus^{tr12} mutant intestinal tubes are devoid of folds in zones 2 and 3, corresponding to the anterior intestine. The differences in structure were restricted to, and specific for, zones 2 and 3; there were no structural differences in zone 4 and no brush border defects observed in the kus^{tr12} embryos, as their enterocytes maintained the expression and localization of 4e8, the absorptive cell marker.

Given these phenotypes, we proceeded to test the functionality of the alleles discovered in our cohort. In family A, the proband was a compound heterozygote for p.Arg262* and p.Val423Asp, the first mutation being considered to encode a null allele. We therefore modeled c.1268T>A (p.Val423Asp). To reduce the phenotypic variability that we have sometimes found in morphants, we focused our studies on the of kus^{tr12} homozygous mutants. Specifically, we injected both human wild-type (WT) and c.1268T>A (p.Val423Asp) encoding mRNA into kus^{tr12} embryos at the 1- to 4-cell stage and we assessed their ability to improve the structural phenotypes observed in zone 2 of 5 dpf mutant guts. Injection of WT human mRNA was able to ameliorate the observed fold defects. In contrast, human c.1268T>A (p.Val423Asp) mRNA-injected kus^{tr12} larvae were 3.44 times more likely to have no folds in zone 2 than kus^{tr12} mutants injected with WT mRNA (Figure 5, $p = 0.005$; OR = 3.441), with modest overall amelioration of the mutant phenotype. Human WT mRNA was unable to rescue zone 3, likely because it forms somewhat later in development, at which point the injected mRNA is mostly extinguished, while zone 4 gave no pathology in mutants and therefore served as an indirect quality control for specificity. Taken together, these data suggested that *UNC45A* plays a role in the development of a functional intestinal system and that the *UNC45A* variant c.1268T>A identified in family A likely results in minimal (but not fully extinguished) UNC45A activity.

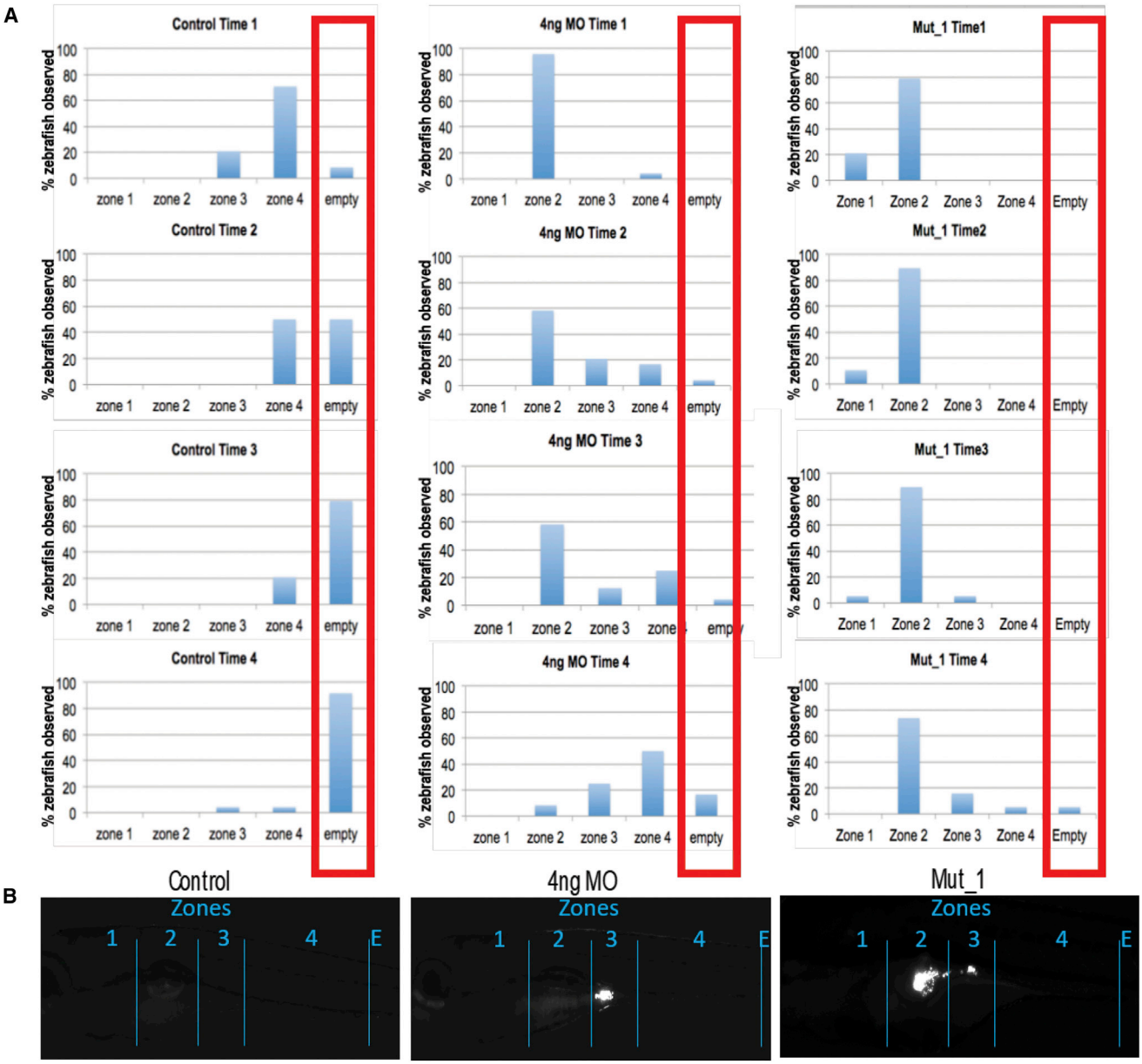

Figure 3. Microgavage Assay to Assess Intestinal Motility
Fluorescent microspheres were gavaged and their transit was observed at 0, 3, 6, 9, and 24 hr in *unc45* morphants and mutants.
(A) Numbers of embryos with observed fluorescence in the four zones of the alimentary canal at four different time points. Compared to controls (left set), in which fluorescent beads peak in zone 4 at time 1 and the progressively expelled from the gut (times 2–4). Both morphants (middle set) and mutants (right set) show presence of fluorescent beads in zones 1 and 2 of the gut.
(B) Representative images of the gut from controls, morphants, and mutants, demarcating the four zones and showing characteristic evidence of GFP in zones 2 and 3.

Discussion

We report a constellation of phenotypes that we propose to represent a distinct clinical entity, osteo-oto-hepato-enteric syndrome (O2HE). The main clinical features of O2HE syndrome include congenital diarrhea, congenital cholestasis, bone fragility, and deafness. In our families' exomes, no mutations were found in genes previously known to be involved in cholestasis, brittle bones, or chronic diarrhea. Together, our *in vitro* and *in vivo* data provide strong evidence that loss of UNC45A function results in a clinical pathology, which includes loss of normal digestive intestinal transit.

Based on current knowledge, there is no obvious link between the clinical expression observed in the affected individuals in the three families and UNC45A function. Most studies of *unc45* have been performed in *Caenorhabditis elegans*. However, invertebrates have a single *unc-45* gene that is expressed in both muscle and non-muscle tissues, whereas vertebrates possess one gene expressed in striated

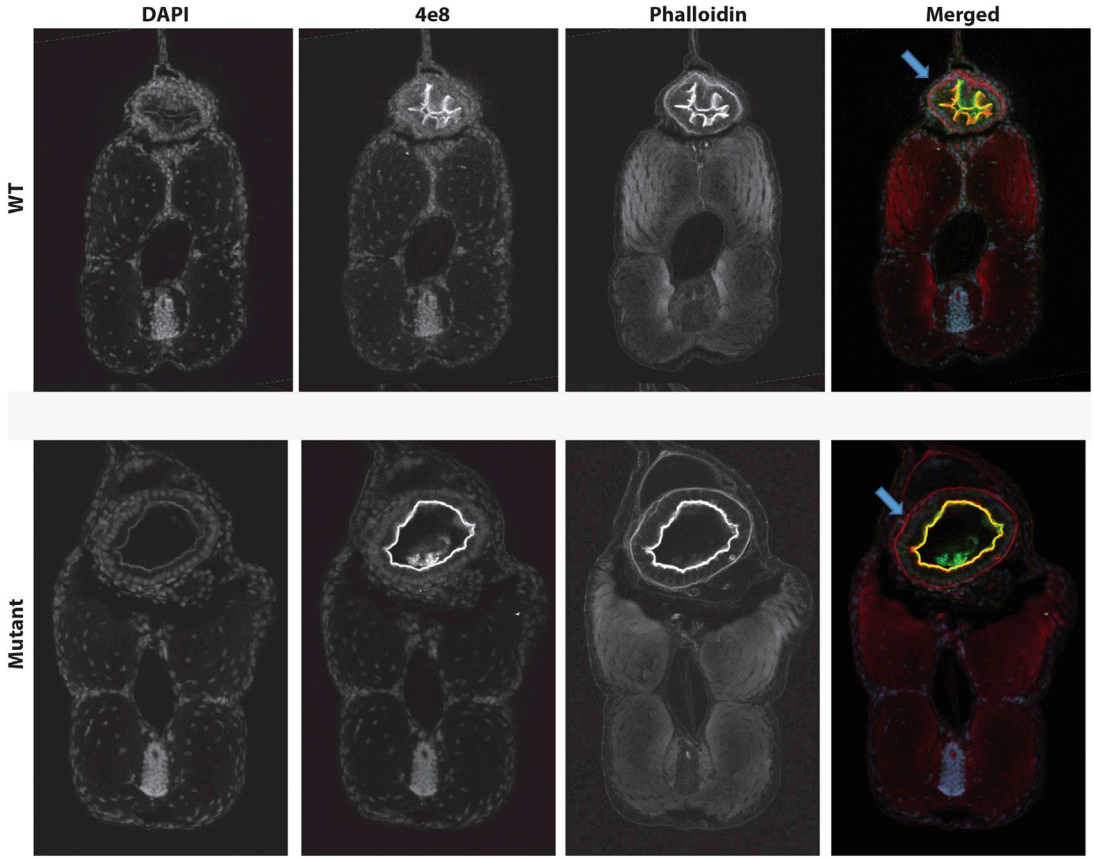

Figure 4. Histological Study of Transverse Sections of Zones 2 and 3 of 5 dpf Zebrafish
Markers for F-actin (Phalloidin) and intestinal brush borders (4e8) were used and revealed defects (lack of epithelial folds in the intestinal tube) in the structure of kus^{tr12} larvae compared to controls.

muscle (*UNC45B*) and another that is expressed more ubiquitously (*UNC45A*). In fact, the phylogeny of UNC-45 homologs showed that this protein family appeared in the Holozoa lineage (Figure S4) and has undergone a duplication event in an ancestor of vertebrates. This event allowed the specialization of the two resulting paralogs: the muscle Unc45B and ubiquitous Unc45A. This divergence might explain the absence of skeletal muscle pathology in the three families studied here, although additional affected individuals will be required to define the full range of the clinical pathologies associated with *UNC45A* mutations in humans.

UNC45A belongs to the UCS protein family (UNC-45/CRO1/She4p). *C. elegans unc-45* was first described after a screening for mutations causing motility disorders (UNC stands for uncoordinated).[24] The UNC-45 protein has three recognizable domains: an N-terminal tetratricopeptide repeat (TRP) domain (~115 amino acids), a central domain of ~400 amino acids, and a C-terminal UCS domain (~400 amino acids).[24,25] The TPR domain participates in protein-protein interactions, especially with Hsp70 (HSPA1A) and Hsp90 HSP90AA1.[26] The role of the central domain remains unclear, while the C-terminal UCS domain is critical for myosin binding.[25] Whether or not variants located within specific domains of UNC45A lead to different functional outcomes is still unknown. UNC45A appears to be ubiquitously expressed and has been postulated to be involved in cytoskeletal functions, such as cell division or exocytosis.[27,28] These data are consistent with the multi-organ defects observed in our affected individuals, as well as the structural pathology in the gut of our zebrafish mutants. However, other features of the protein are not reflected in the phenotype seen in humans. For example, UNC45A co-localizes with type II muscle myosin heavy chain B as well as type V myosins and plays an essential role in myoblast fusion and cell proliferation.[29–32] However, none of our affected individuals present muscular alterations, none have muscle weakness, and all present normal creatine phosphokinase level. Recently, *in vivo* studies have reported that *unc45a* plays a role in aortic arch development and could be one underlying cause of human vessel malformations.[23] This, coupled to reports that individuals with visceral arteriovenous malformations can be more susceptible to cholestasis,[33] makes UNC45A an attractive candidate; however, none of the people in our study display vessel malformation. Although this might be due to differences in development and physiology between lower organisms and humans, we favor the hypothesis in which minimal activity of the human alleles (in contrast to null homozygous

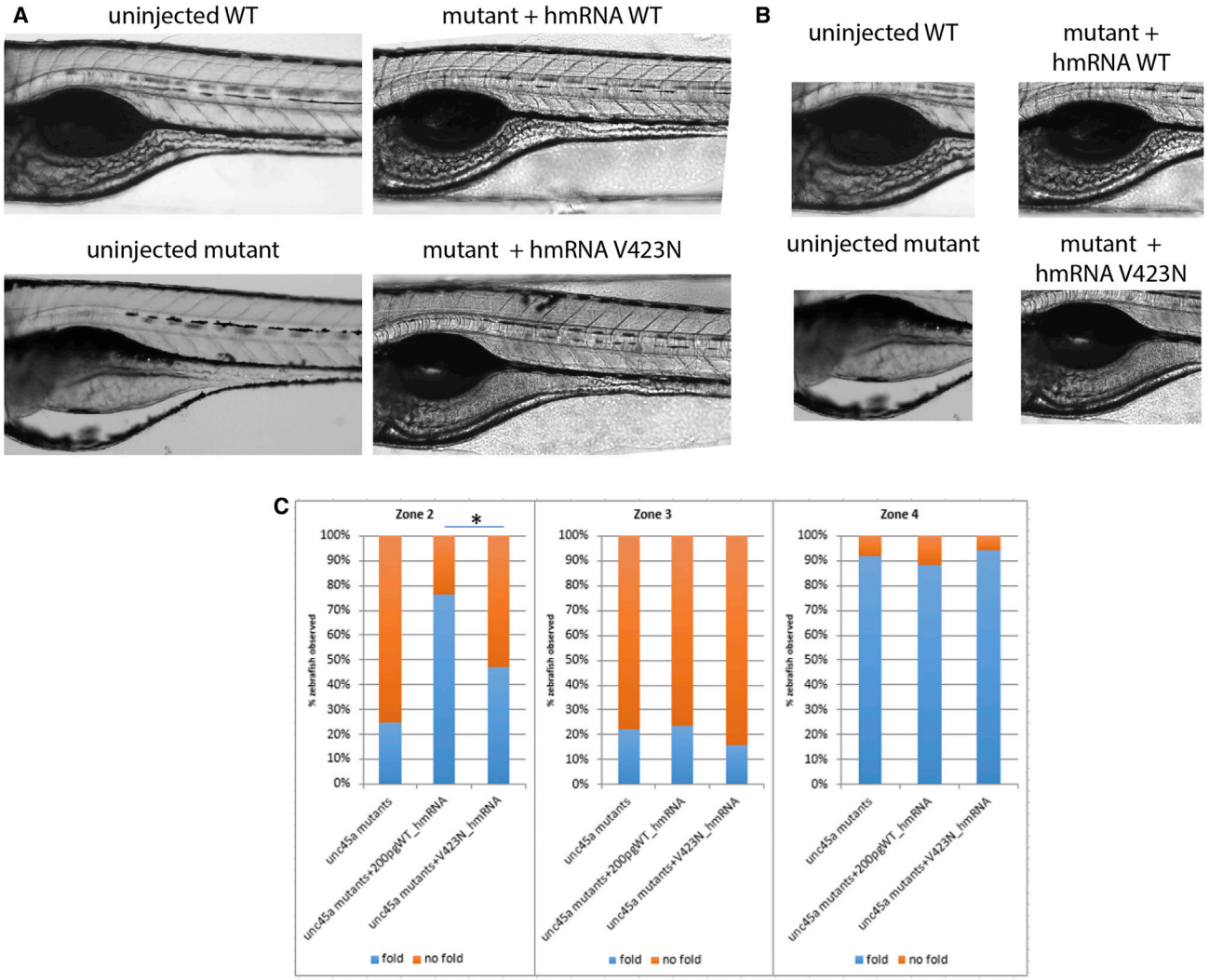

Figure 5. Assessment of Human UNC45A c.1268T>A, Resulting in a p.Val423Asp Change (V423N), on Zones 2 and 3 of Mutant unc45a Zebrafishes

Mutant embryos were injected with either WT or V423N-encoding mRNA and intestinal folds were observed using brightfield microscopy. Mutants injected with WT encoding mRNA were able to restore folds in zones 2 and 3, but those injected with V423N-encoding mRNA were not restored, illustrating that V423N is pathogenic.

zebrafish embryos) might protect from this pathology. Moreover, even if the link between the observed transit time delay in zebrafish and congenital diarrhea disease is not obvious, prolonged intestinal transit and diarrhea have been already observed in the familial GUCY2C diarrhea syndrome (FGDS), a rare autosomal-dominant inherited disease.[34] More studies are needed to fully understand the physio pathological basis of the diarrhea in O2HE.

The identification of additional mutations at this locus will help clarify these questions.

There is a core phenotype in O2HE syndrome: four main signs seen in at least three individuals (Figure 1C). Phenotypic variability is observed in the three families studied here; however, this is seen in other congenital diseases (for example microvillus inclusion disease or tricho-hepato-enteric syndrome) and is expected in such complex diseases. The four individuals present some degree of developmental delay but we can't exclude that it is a non-specific symptom. Indeed, in the individuals A.II.2, B.II.3, and B.II.4, the delay could be a secondary effect of the deafness. There are also some isolated signs, such as the tubulopathy and poor glycemic regulation found in individual C.II.1 and the hydrocephalus-related to stenosis of the aqueduct of Sylvius and the vesico-ureteral reflux found in individual B.II.4. It remains unclear whether these isolated signs are related to *UNC45A* or not. The clinical heterogeneity could reflect differing degrees of functional deficiency resulting from distinct effects of each mutation on UNC45A expression/stability on different tissues. Although we observe similar protein levels in lymphoblastoid cells, we cannot exclude that the mutations could have a differential impact on specific tissues. We also do not have direct evidence that all the mutations in

the reported families undergo nonsense-mediated decay; further studies will be necessary to determine whether this mutational mechanism is ubiquitous. The variable expressivity could also be impacted by modifiers, epigenetics, or environmental factors.

In conclusion, our study finds a strong association between *UNC45A* loss-of-function mutations and a syndrome, we named osteo-oto-hepato-enteric (O2HE) syndrome. According to previous reports, *UNC45A* is possibly associated with the cytoskeleton and further evidence needs to be accumulated to understand the molecular mechanisms underlying the O2HE syndrome.

Supplemental Data

Supplemental Data include ten figures, two movies, and Supplemental Note (case reports) and can be found with this article online at https://doi.org/10.1016/j.ajhg.2018.01.009.

Acknowledgments

We are grateful to all the affected individuals and their families who participated in this study. We would like to thank Beth Roman for sharing the kurzschlusstr12 zebrafish, Jennifer Bagwell and Michel Bagnat for their expert advice on intestinal phenotyping and antibodies, and Melanie Garrett and Allison Ashley-Koch for their assistance with the statistical analysis of the zebrafish work. We also thank Erica Davis and Michael Mitchell for critical reading of the manuscript and helpful suggestions and Nathalie Colavolpe for her help with X-ray. This work was supported in part by grants from the Fondation Maladies Rares (WES20150601), AMGORE (Association Méditerranéenne pour les Greffes d'ORganes aux Enfants), the Regional Council of Burgundy (PARI 2014), the GFHGNP (Groupe Francophone d'Hépatologie-Gastroentérologie et Nutrition Pédiatriques, "Prix de recherche du Groupe Francophone d'Hépatologie, Gastroentérologie et de Nutrition Pédiatriques 2015"), and the patient support group Association Romy - La vie par un fil.

Received: October 25, 2017
Accepted: January 11, 2018
Published: February 8, 2018

Web Resources

1000 Genomes Browsers, http://www.internationalgenome.org/1000-genomes-browsers/
BMGE, ftp://ftp.pasteur.fr/pub/gensoft/projects/BMGE/
CLUSTAL, https://www.ebi.ac.uk/Tools/msa/clustalo/
Ensembl Genome Browser, http://www.ensembl.org/index.html
ExAC Browser, http://exac.broadinstitute.org/
GenBank, https://www.ncbi.nlm.nih.gov/genbank/
gnomAD Browser, http://gnomad.broadinstitute.org/
ImageJ Fiji, http://fiji.sc/Fiji
MAFFT, https://mafft.cbrc.jp/alignment/software/
Mutalyzer, https://mutalyzer.nl/index
MutationTaster, http://www.mutationtaster.org/
NCBI, https://www.ncbi.nlm.nih.gov/
OMIM, http://www.omim.org/
PolyPhen-2, http://genetics.bwh.harvard.edu/pph2/
UMD-Predictor, http://umd-predictor.eu/
VarAFT http://varaft.eu

References

1. Müller, T., Hess, M.W., Schiefermeier, N., Pfaller, K., Ebner, H.L., Heinz-Erian, P., Ponstingl, H., Partsch, J., Röllinghoff, B., Köhler, H., et al. (2008). MYO5B mutations cause microvillus inclusion disease and disrupt epithelial cell polarity. Nat. Genet. *40*, 1163–1165.
2. Gonzales, E., Taylor, S.A., Davit-Spraul, A., Thébaut, A., Thomassin, N., Guettier, C., Whitington, P.F., and Jacquemin, E. (2017). MYO5B mutations cause cholestasis with normal serum gamma-glutamyl transferase activity in children without microvillous inclusion disease. Hepatology *65*, 164–173.
3. Qiu, Y.L., Gong, J.Y., Feng, J.Y., Wang, R.X., Han, J., Liu, T., Lu, Y., Li, L.T., Zhang, M.H., Sheps, J.A., et al. (2017). Defects in myosin VB are associated with a spectrum of previously undiagnosed low γ-glutamyltransferase cholestasis. Hepatology *65*, 1655–1669.
4. Lapierre, L.A., Kumar, R., Hales, C.M., Navarre, J., Bhartur, S.G., Burnette, J.O., Provance, D.W., Jr., Mercer, J.A., Bähler, M., and Goldenring, J.R. (2001). Myosin vb is associated with plasma membrane recycling systems. Mol. Biol. Cell *12*, 1843–1857.
5. Hales, C.M., Vaerman, J.P., and Goldenring, J.R. (2002). Rab11 family interacting protein 2 associates with Myosin Vb and regulates plasma membrane recycling. J. Biol. Chem. *277*, 50415–50421.
6. Thompson, R.J., and Knisely, A.S. (2014). Microvilli as markers of disordered apical-membrane trafficking and assembly: bowel and liver. Hepatology *60*, 34–36.
7. Girard, M., Lacaille, F., Verkarre, V., Mategot, R., Feldmann, G., Grodet, A., Sauvat, F., Irtan, S., Davit-Spraul, A., Jacquemin, E., et al. (2014). MYO5B and bile salt export pump contribute to cholestatic liver disorder in microvillous inclusion disease. Hepatology *60*, 301–310.
8. Davit-Spraul, A., Fabre, M., Branchereau, S., Baussan, C., Gonzales, E., Stieger, B., Bernard, O., and Jacquemin, E. (2010). ATP8B1 and ABCB11 analysis in 62 children with normal gamma-glutamyl transferase progressive familial intrahepatic cholestasis (PFIC): phenotypic differences between PFIC1 and PFIC2 and natural history. Hepatology *51*, 1645–1655.
9. Pawlikowska, L., Strautnieks, S., Jankowska, I., Czubkowski, P., Emerick, K., Antoniou, A., Wanty, C., Fischler, B., Jacquemin, E., Wali, S., et al. (2010). Differences in presentation and progression between severe FIC1 and BSEP deficiencies. J. Hepatol. *53*, 170–178.
10. Fabre, A., Charroux, B., Martinez-Vinson, C., Roquelaure, B., Odul, E., Sayar, E., Smith, H., Colomb, V., Andre, N., Hugot, J.P., et al. (2012). SKIV2L mutations cause syndromic diarrhea, or trichohepatoenteric syndrome. Am. J. Hum. Genet. *90*, 689–692.
11. Monies, D.M., Rahbeeni, Z., Abouelhoda, M., Naim, E.A., Al-Younes, B., Meyer, B.F., and Al-Mehaidib, A. (2015). Expanding phenotypic and allelic heterogeneity of tricho-hepato-enteric syndrome. J. Pediatr. Gastroenterol. Nutr. *60*, 352–356.
12. Rider, N.L., Boisson, B., Jyonouchi, S., Hanson, E.P., Rosenzweig, S.D., Cassanova, J.L., and Orange, J.S. (2015). Novel TTC37 mutations in a patient with immunodeficiency without diarrhea: extending the phenotype of trichohepatoenteric syndrome. Front Pediatr. *3*, 2.

13. Thevenon, J., Milh, M., Feillet, F., St-Onge, J., Duffourd, Y., Jugé, C., Roubertie, A., Héron, D., Mignot, C., Raffo, E., et al. (2014). Mutations in SLC13A5 cause autosomal-recessive epileptic encephalopathy with seizure onset in the first days of life. Am. J. Hum. Genet. *95*, 113–120.
14. Davis, E.E., Frangakis, S., and Katsanis, N. (2014). Interpreting human genetic variation with in vivo zebrafish assays. Biochim. Biophys. Acta *1842*, 1960–1970.
15. Cocchiaro, J.L., and Rawls, J.F. (2013). Microgavage of zebrafish larvae. J. Vis. Exp., e4434.
16. Bonora, E., Bianco, F., Cordeddu, L., Bamshad, M., Francescatto, L., Dowless, D., Stanghellini, V., Cogliandro, R.F., Lindberg, G., Mungan, Z., et al. (2015). Mutations in RAD21 disrupt regulation of APOB in patients with chronic intestinal pseudo-obstruction. Gastroenterology *148*, 771–782.e11.
17. Bainbridge, M.N., Davis, E.E., Choi, W.Y., Dickson, A., Martinez, H.R., Wang, M., Dinh, H., Muzny, D.M., Pignatelli, R., Katsanis, N., et al. (2015). Loss of function mutations in NNT are associated with left ventricular noncompaction. Circ Cardiovasc Genet *8*, 544–552.
18. Salgado, D., Desvignes, J.P., Rai, G., Blanchard, A., Miltgen, M., Pinard, A., Lévy, N., Collod-Béroud, G., and Béroud, C. (2016). UMD-Predictor: a high-throughput sequencing compliant system for pathogenicity prediction of any human cDNA substitution. Hum. Mutat. *37*, 439–446.
19. Frédéric, M.Y., Lalande, M., Boileau, C., Hamroun, D., Claustres, M., Béroud, C., and Collod-Béroud, G. (2009). UMD-predictor, a new prediction tool for nucleotide substitution pathogenicity – application to four genes: FBN1, FBN2, TGFBR1, and TGFBR2. Hum. Mutat. *30*, 952–959.
20. Lehtimäki, J.I., Fenix, A.M., Kotila, T.M., Balistreri, G., Paavolainen, L., Varjosalo, M., Burnette, D.T., and Lappalainen, P. (2017). UNC-45a promotes myosin folding and stress fiber assembly. J. Cell Biol. *216*, 4053–4072.
21. Sugathan, A., Biagioli, M., Golzio, C., Erdin, S., Blumenthal, I., Manavalan, P., Ragavendran, A., Brand, H., Lucente, D., Miles, J., et al. (2014). CHD8 regulates neurodevelopmental pathways associated with autism spectrum disorder in neural progenitors. Proc. Natl. Acad. Sci. USA *111*, E4468–E4477.
22. Bernier, R., Golzio, C., Xiong, B., Stessman, H.A., Coe, B.P., Penn, O., Witherspoon, K., Gerdts, J., Baker, C., Vulto-van Silfhout, A.T., et al. (2014). Disruptive CHD8 mutations define a subtype of autism early in development. Cell *158*, 263–276.
23. Anderson, M.J., Pham, V.N., Vogel, A.M., Weinstein, B.M., and Roman, B.L. (2008). Loss of unc45a precipitates arteriovenous shunting in the aortic arches. Dev. Biol. *318*, 258–267.
24. Venolia, L., Ao, W., Kim, S., Kim, C., and Pilgrim, D. (1999). unc-45 gene of *Caenorhabditis elegans* encodes a muscle-specific tetratricopeptide repeat-containing protein. Cell Motil. Cytoskeleton *42*, 163–177.
25. Barral, J.M., Bauer, C.C., Ortiz, I., and Epstein, H.F. (1998). Unc-45 mutations in *Caenorhabditis elegans* implicate a CRO1/She4p-like domain in myosin assembly. J. Cell Biol. *143*, 1215–1225.
26. Scheufler, C., Brinker, A., Bourenkov, G., Pegoraro, S., Moroder, L., Bartunik, H., Hartl, F.U., and Moarefi, I. (2000). Structure of TPR domain-peptide complexes: critical elements in the assembly of the Hsp70-Hsp90 multichaperone machine. Cell *101*, 199–210.
27. Price, M.G., Landsverk, M.L., Barral, J.M., and Epstein, H.F. (2002). Two mammalian UNC-45 isoforms are related to distinct cytoskeletal and muscle-specific functions. J. Cell Sci. *115*, 4013–4023.
28. Iizuka, Y., Cichocki, F., Sieben, A., Sforza, F., Karim, R., Coughlin, K., Isaksson Vogel, R., Gavioli, R., McCullar, V., Lenvik, T., et al. (2015). UNC-45A is a nonmuscle myosin IIA chaperone required for NK cell cytotoxicity via control of lytic granule secretion. J. Immunol. *195*, 4760–4770.
29. Bazzaro, M., Santillan, A., Lin, Z., Tang, T., Lee, M.K., Bristow, R.E., Shih, IeM., and Roden, R.B. (2007). Myosin II co-chaperone general cell UNC-45 overexpression is associated with ovarian cancer, rapid proliferation, and motility. Am. J. Pathol. *171*, 1640–1649.
30. Kachur, T., Ao, W., Berger, J., and Pilgrim, D. (2004). Maternal UNC-45 is involved in cytokinesis and colocalizes with nonmuscle myosin in the early *Caenorhabditis elegans* embryo. J. Cell Sci. *117*, 5313–5321.
31. Venolia, L., and Waterston, R.H. (1990). The *unc-45* gene of *Caenorhabditis elegans* is an essential muscle-affecting gene with maternal expression. Genetics *126*, 345–353.
32. Ao, W., and Pilgrim, D. (2000). *Caenorhabditis elegans* UNC-45 is a component of muscle thick filaments and colocalizes with myosin heavy chain B, but not myosin heavy chain A. J. Cell Biol. *148*, 375–384.
33. Lerut, J., Orlando, G., Adam, R., Sabbà, C., Pfitzmann, R., Klempnauer, J., Belghiti, J., Pirenne, J., Thevenot, T., Hillert, C., et al.; European Liver Transplant Association (2006). Liver transplantation for hereditary hemorrhagic telangiectasia: Report of the European liver transplant registry. Ann. Surg. *244*, 854–862, discussion 862–864.
34. von Volkmann, H.L., Brønstad, I., Gilja, O.H., R Tronstad, R., Sangnes, D.A., Nortvedt, R., Hausken, T., Dimcevski, G., Fiskerstrand, T., and Nylund, K. (2017). Prolonged intestinal transit and diarrhea in patients with an activating GUCY2C mutation. PLoS ONE *12*, e0185496.

The American Journal of Human Genetics, Volume *102*

Supplemental Data

Loss-of-Function Mutations in *UNC45A* Cause a Syndrome Associating Cholestasis, Diarrhea, Impaired Hearing, and Bone Fragility

Clothilde Esteve, Ludmila Francescatto, Perciliz L. Tan, Aurélie Bourchany, Cécile De Leusse, Evelyne Marinier, Arnaud Blanchard, Patrice Bourgeois, Céline Brochier-Armanet, Ange-Line Bruel, Arnauld Delarue, Yannis Duffourd, Emmanuelle Ecochard-Dugelay, Géraldine Hery, Frédéric Huet, Philippe Gauchez, Emmanuel Gonzales, Catherine Guettier-Bouttier, Mina Komuta, Caroline Lacoste, Raphaelle Maudinas, Karin Mazodier, Yves Rimet, Jean-Baptiste Rivière, Bertrand Roquelaure, Sabine Sigaudy, Xavier Stephenne, Christel Thauvin-Robinet, Julien Thevenon, Jacques Sarles, Nicolas Levy, Catherine Badens, Olivier Goulet, Jean-Pierre Hugot, Nicholas Katsanis, Laurence Faivre, and Alexandre Fabre

Supplemental Data

Supplemental Case report

Family A

The proband is a 5-year-old girl, the second child of healthy unrelated parents with no family history of digestive disease. There were no significant medical events her father's family or in her sister. The proband was born at term after an uneventful pregnancy by elective caesarean section. Birth weight was 2.980 g (-1 standard deviation (SD)), length was 46 cm (-2.5 SD) and occipital-frontal-circumference was 32 cm (-2.5 SD). Dehydration linked to severe profuse hydric diarrhea occurred from the fouth day of life leading to a weight loss of 20%. Initial explorations showed a secretory diarrhea profile with no evidence of infectious, immunologic or thyroid disease. There was no evidence of malabsorption or exudative enteropathy. The osmole gap and ionic stool concentration showed a rather secretory profile of the diarrhea. The carmine red test revealed a dramatic increase in intestinal transit time. Oral feeding with high degree cows' milk protein hydrolysate and enteral nutrition failed to improve the digestive leaks and exclusive parenteral nutrition was started. Endoscopic explorations with repeated intestinal biopsies using the periodic acid–Schiff showed focal abnormalities of the brush border which could be evocative of atypical microvillus inclusion disease. No tufting brush border was discovered during the pathology examination. Liver exploration was normal. Conjunctive biopsy did not show the presence of tufts. The hypothesis of a potential endocrine secreting tumor was ruled out by imaging and biochemical assays. In order to look for malformations associated with the digestive phenotype, cardiac ultrasound and MRI were performed but revealed no abnormalities. Immune and metabolic explorations were negative.

Nutritional management was marked by cyclization difficulties of parenteral nutrition and the impossibility to restart enteral feeding. Persistent hypokalemia was treated with supplementation, and chronic anemia with repeated iron infusions. The evolution was marked by language delay linked to severe bilateral deafness, which appeared during evolution, without psychomotor retardation. Growth retardation was only moderate thanks to regular adaptation of parenteral nutritional intake. Targeted sequencing of the *MYO5B* gene was negative. There was no history of bone frailty and DXA performed at age 4 years was normal. She has no muscle weakness and present normal Creatine Phosphokinase level.

Family B

Patient B.II.3

Patient B.II.3 is the third of four children, born at 38 weeks of gestation and is currently 23 years old. At 15 days of life she presented with neonatal jaundice with normal level of GGT associated with pale stools, dark urine and stagnation weight. Initial diagnosis was a Byler disease because of the association of a cholestasis with a persistent jaundice with normal GGT, elevated level of serum bile acids and some level of fibrosis on a liver biopsy performed at 10 months of life. On the clinical and biological levels, bilirubin levels returned to normal at 2.5 years of age. However major pruritus persisted with elevated serum bile acid, leading to partial internal biliary diversion for intractable pruritus at the age of 19. Surgery allowed for a decrease of the serum bile acid and a transient decrease of the pruritus.

The proband also presented with multiple fractures (23 during a period of 23 years) with no biological deficiency of D vitamin. The osteodensitometry test (bone density scan) at 20 years showed a whole body bone densitometry (BDM) with a T-score at -

2.9 and a Z-score at -1.5. Another at 24 years showed a vertebra BDM T-score of -3 and Z-score of -2.4 and femora BDM T-score of -0.9 and a Z-score of -0.6. Additionally, she had bilateral perception hearing loss diagnosed around the age of 5 years. The development of her language was poor and she presented with mild intellectual disability with a delay of acquisitions. She also had muscular inter ventricular communication, diagnosed at the neonatal period which resolved spontaneously, and a persistent asthma (treated). On the digestive level, she had a diverse food regimen and no diarrhea though her growth was restricted. She has a current weight of 38.5 kg and height of 147.5 cm.

Patient B.II.4

Patient B.II.4 is the fourth child, born at term and eutrophic, currently 18 years old. At 7 days, she presented with cholestasis with elevated GGT (Gamma Glutamyl Transaminases) up to 21 times normal values, resolving by the age of 3. Similar to her sister, a significant pruritus persisted, leading to a bypass surgery cholecysto-jejunocolostomy at the age of 12 years. The improvement was temporary, and itching and increased bile acid persists. On the digestive level, there is a syndrome of food intolerance with very early onset of diarrhea and failure to thrive requiring the introduction of parenteral nutrition and enteral feeding in combination with diversified regimen in small quantities. Diarrhea spontaneously resolved with time. Endoscopy was performed at the age of 1 year, because of a non-specific aspect of villous atrophy on intestine. At the age of 17, she presented a severe acute gastroenteritis due to Salmonella complicated by Clostridium infection when returning from Tunisia, with a very severe dehydration leading to hospitalization in resuscitation unit. Since then, the stools remain liquid, sometimes slimy but not bleeding, accompanied by

intermittent abdominal pain relieved by issuing stools. As her sister, she presented severe bone fragility, also with multiple fractures (Figure S6) and osteonecrosis of the femoral head at the age of 14 years, secondary to left hip dysplasia at birth (Figure S5). On the growth plan, we also reported a significant failure to thrive. Initially, hearing assessments have reported a normal hearing. Perception deafness needing hearing aid was diagnosed in adolescence. Neurologically, she presented a prenatal diagnosis of hydrocephalus related to stenosis Silvius aqueduct. She therefore received a ventricular-peritoneal shunt at the age of 4 months, removed 13 years later because of poor tolerance. She presented psychomotor retardation with delayed language and scored acquisitions, necessitating her management in Medical Educational Institute. On the urological plan vesico-ureteral reflux stage II was diagnosed at the age of 1 year, spontaneously evolving favorably. No anomaly was noted in the heart and breathing plan. The growth remains poor with at last evaluation a weight of 38.5kg (-3SD) and a height of 147.5cm (-2.5SD).

For these 2 children, geneticists reported the plane dysmorphic blue sclera, abnormalities of the extremities, malocclusions, the watch glass nails. There was no muscular weakness with normal CPK and both have normal puberty. Diverse genetic explorations were performed with a CGH array dismissing a chromosome rearrangement and direct sequencing of *ATP8B1* [MIM: 602397] and *ABCB11* [MIM: 603201] implicated in Progressive Familial Intrahepatic Cholestasis-1 (PFIC1 [MIM: 211600]) and 2 respectively (PFIC-2 [MIM: 601847]) and of *VPS33b* [MIM: 608552] implicated in arthrogryposis, renal dysfunction, and cholestasis 1 (ARC syndrome [MIM: 208085]) was normal.

Furthermore, immunolabeling experiments on liver biopsies show mislocalization of hepatic canalicular proteins (such as ABCB11, CD13 and GGT1) (Figure S1, S2). This suggests that *UNC45A* is involved in the distribution of these proteins in the cell, although the underlying mechanisms are unknown.

Reassessment of liver pathology in Family B (Figure S1)

The patient B.II.3 a liver biopsy was taken at the age of 19 years. Histologically, the liver architecture was preserved and there was no clear sign of fibrosis. The portal tracts showed a discrete ductular reaction with inflammation. Bile duct damage was not clearly identified. In the parenchyma, there was no sign of lobular inflammation or steatosis as view by immunohistochemistry. The Aminopeptidase N, CD13 showed a canalicular expression in the hepatocytes and an apical expression in the bile ducts, ABCB11 a canalicular expression in the hepatocytes and ABCC2 (ATP-binding cassette, subfamily c, member 2, also called MRP2) a canalicular expression in the hepatocytes. However, sequencing of *ABCB4* (also called *MDR3* for Multi-Drug Resistant 3) involved in PFIC3 [MIM: 602347]) and GGT1 (gamma-glutamyltransferase1) showed no mutation (Figure S1).

For the patient B.II.4, the liver biopsy was sampled at the age 12 years. The liver architecture was preserved, however, it showed a pericellular fibrosis, periductal fibrosis in the portal tracts, and ballooned hepatocytes with occasionally Mallory denk body indicating a (fibrosing) cholestatic pathology. Immunohistochemically, MDR3 and GGT1 were negative in the hepatocytes, whereas canalicular ABCB11, ABCC2, and CD13 immunoreactivity in the hepatocytes was identified (Figure S1).

Family C

The proband is 5 years old girl. She was born to healthy unrelated parents of Turkish origin. The father is carrier of a Polyglobulia. The pregnancy was uneventful. Birth occurred at term 41 weeks, Birth weight: 2800g, Height 49.5 cm, Head circumference: 32 cm.

At 1 month, she was admitted in a tertiary center for jaundice and a failure to thrive. Investigations showed no evidence for usual causes of cholestasis. At nearly 2 months of age, because stools were partially discolored, a transvesicular cholangiography was performed which showed a normal biliary tree. A Liver biopsy performed in the same time showed: severe hepatocellular cholestasis, giant cell transformation, micro vesicular steatosis (20%), portal fibrosis and lobular fibrosis without septa. There was no ductular reaction or bile duct paucity. In addition she presented with severe watery diarrhea, vomiting (improving by fasting), spontaneous ileo-ileal invaginations twice, a tubulopathy with hyperdiurese, proteinuria, acidosis he whole leading to a failure to thrive.

Because of the severe undernutrition (4.4kg at 5 months) a parenteral nutrition was settled at the age of 6 months, which allowed the normalization of the growth although the diarrhea persisted as well as intermittent tubulopathy and cytolysis.

At six months of life she presented a bone demineralization without evidence of rickets or imperfecta osteogenesis and two severe spontaneous fractures occurred (tibia and femur) when she was 2.

There was no neurologic deficit, and no hearing deficit (hearing tests PEA and OEA positive). There was slight developmental delay but no autistic traits to date.

The probands present a small facial dimorphism with large forehead, but no hair changes nor cutaneous spots.

Intestinal biopsies found a partial and mild villous atrophy with brush border abnormalities with no argument for celiac disease. The *MYO5B* gene was normal as well as the genes of the tricho-hepato-enteric syndrome (THES1 [MIM: 222470]; THES2 [MIM: 614602]) *TTC37* [MIM: 614589] and *SKIV2L* [MIM: 600478]. Fecal elastase was normal. During the follow up, the child remains under parenteral nutrition till now (5 years) but oral alimentation has been initiated (around 3 years of age) without increasing the stool output but did not allow the complete weaning of parenteral nutrition.

During the course of the follow up the evolution was marked by episodes of increased stool output, tubulopathy with proteinuria, all contributing to dehydration, and fluctuant cytolysis without oubvious starting event . She experienced very few infectious events.

Although the bone demineralization remained unchanged, she did not experience other fractures nor complained about bone pain. The calcium- phosphorus balance, D vitamin and PTH remained normal except during the acute phases of tubulopathy.

She has no muscle weakness and all present normal Creatine Phosphokinase level.

Recently she developed a poor glycemic regulation requiring insulin therapy, but the mechanism is so far unclear. She is still under parenteral nutrition.

Supplemental figures and legends

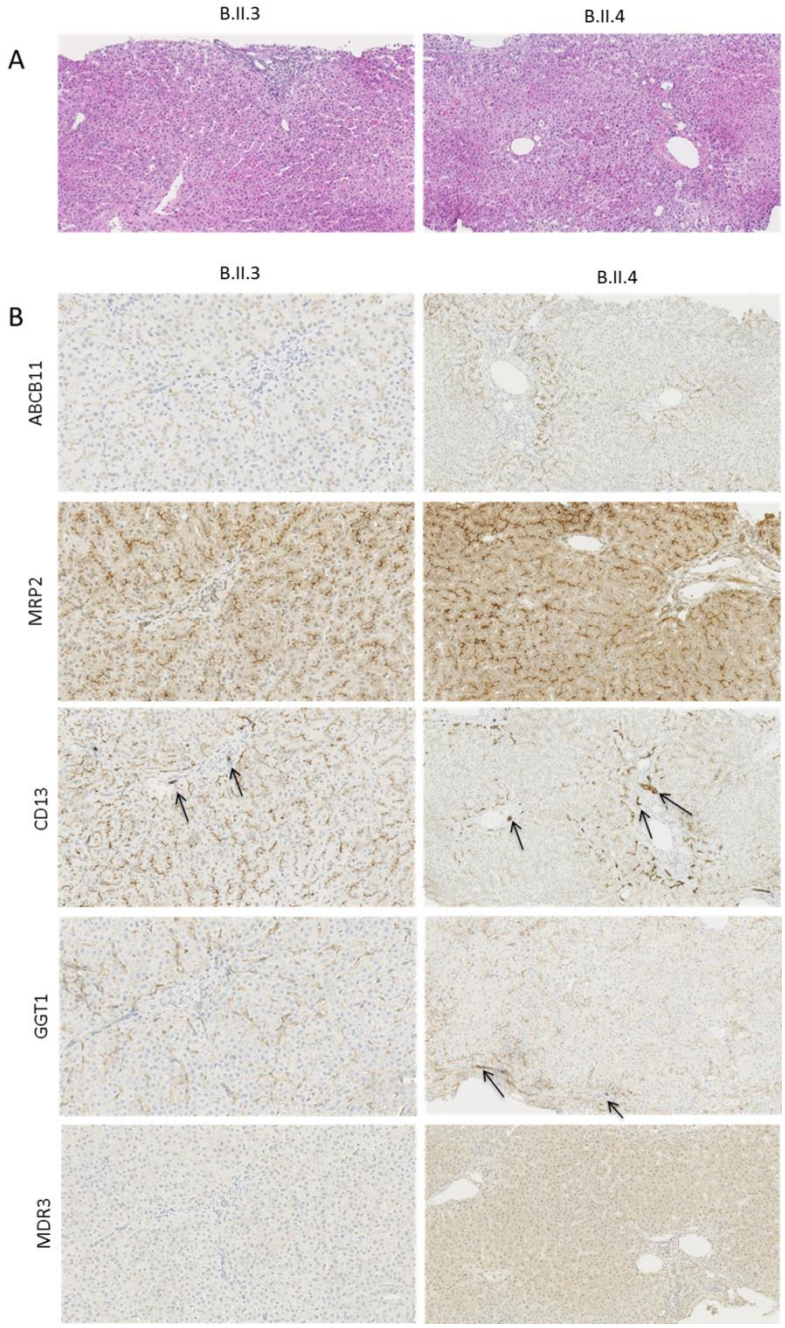

Figure S1: Photomicrographs and immunolabeling on liver biopsies of the Family B patients at 19 and 12 years respectively.

(A) Photomicrographs of patients B.II.3 and B.II.4. Individual B.II.3: Liver architecture is preserved. No clear sign of fibrosis. Portal tracts: discrete ductular reaction with inflammation. No biliary damage. Parenchyme: no steatosis. No cholestatic feature. No ballooned hepatocytes. Patient B.II.4: Liver architecture is preserved; however, it shows (fibrosing) cholestatic pathology, such as pericellular fibrosis, periductal fibrosis in the portal tracts, ballooned hepatocytes with occasionally mallory denk body. (B) Immunolabbeling. Patient B.II.3 CD13: canalicular expression in the

hepatocytes. Apical expression in the bile ducts (arrow); ABCB11: canalicular expression in the hepatocytes; GGT1: negative; MRP2: canaliculare expression in the hepatocytes. Patient B.II.4: ABCB11: deletion of the canalicular expression in the hepatocytes; CD13: deletion of the canalicular expression in the hepatocytes, however, apical expression of the bile ducts is preserved (arrow); GGT1: absence of the canalicular expression in the hepatocytes, however, apical expression of the bile ducts is preserved (arrow); MRP2 (normal pattern): canalicular expression in the hepatocytes and apical expression in the bile ducts (arrow).

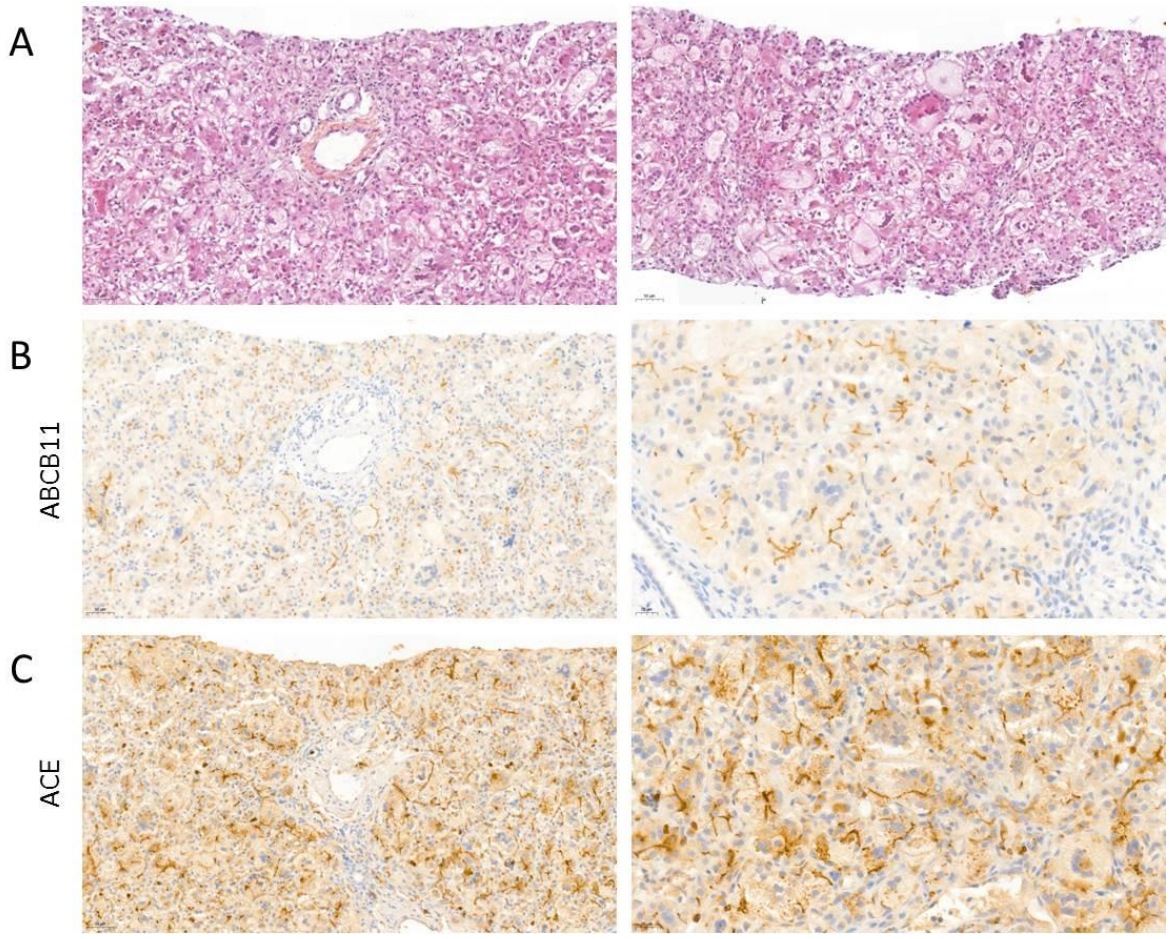

Figure S2: Photomicrographs and immunolabeling on liver biopsies of the patient C.II.1

(A) Photomicrographs of patients C.II.1 Hematoxylin and eosin staining showing hepatocellular, canalicular cholestasis, giant cell transformation of hepatocytes, microvesicular steatosis (20%), slight portal and lobular fibrosis.(B) Immunolabelling. Patient C.II.1 BSEP: canalicular expression is conserved, however a thickened canalicular staining is observed.

(C) Immunolabelling. Patient C.II.1 ECA: canalicular expression is conserved, however, a thickened canalicular staining and a granular and patchy pattern in the subcanalicular area is observed

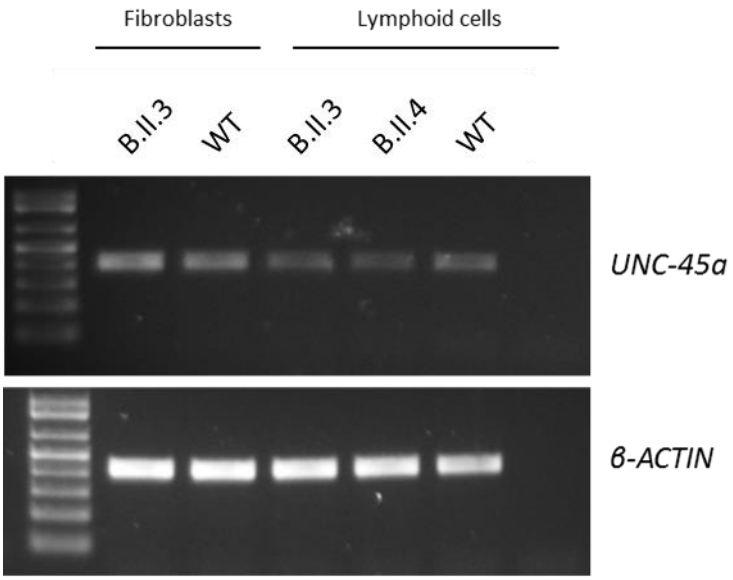

Figure S3: Detection of UNC45A transcripts by reverse transcription-PCR using mRNA of patients (Family B) and WT fibroblasts and lymphoid cells

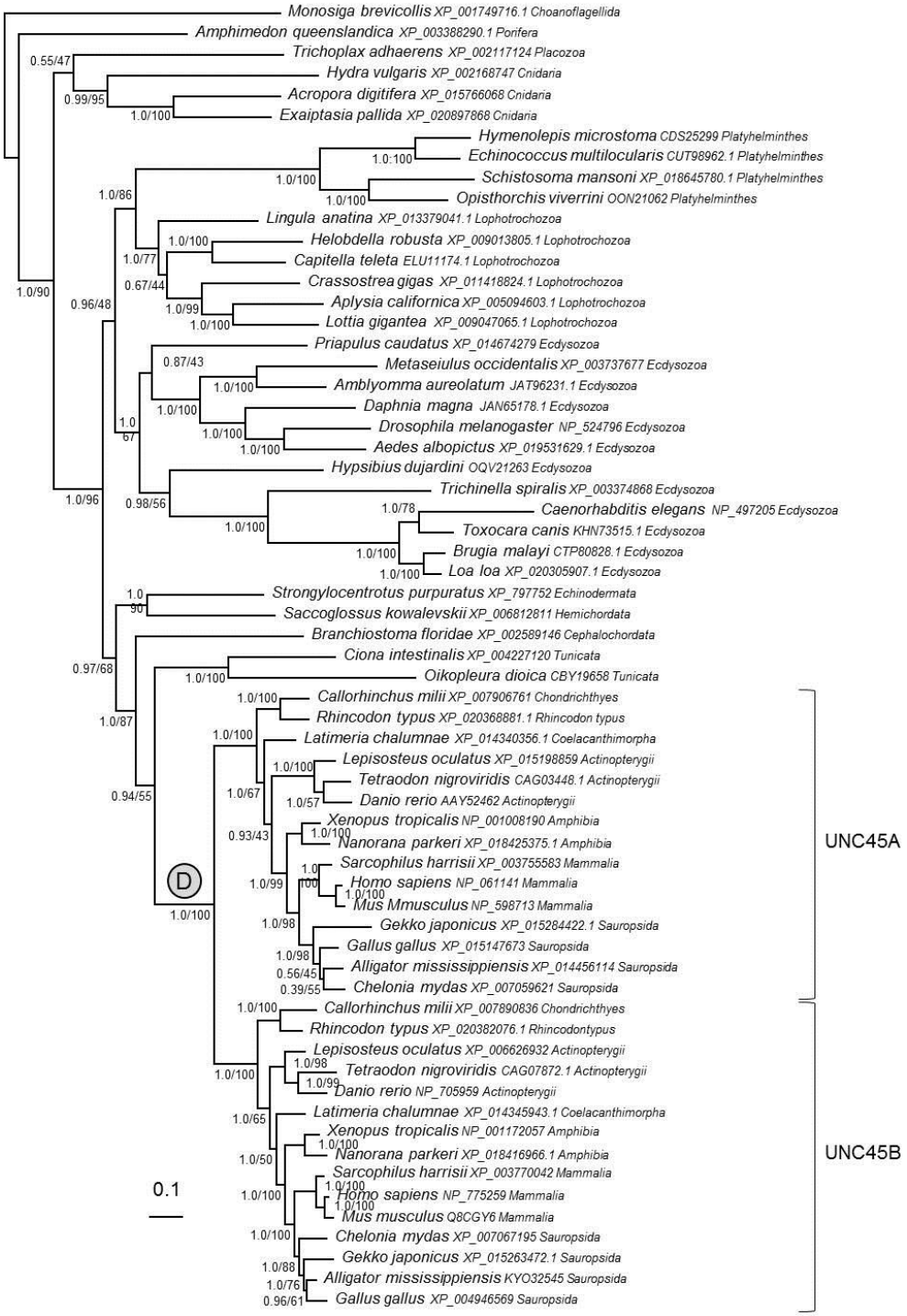

Figure S4: Bayesian tree of metazoan UNC45/UNC45A/UNC45B proteins (63 sequences, 704 amino acid positions).

The tree is rooted with the sequence of *Monosiga brevicollis* (Choanoflagellida), a close relative of animals. Numbers at branches correspond to posterior probabilities / bootstrap values. Values greater than 0.95/ 90% correspond to strongly supported branches. The scale bar indicates the average number of substitutions per site. A duplication event, indicated by a circle, occurred in branch leading to the last common ancestor of Vertebrata.

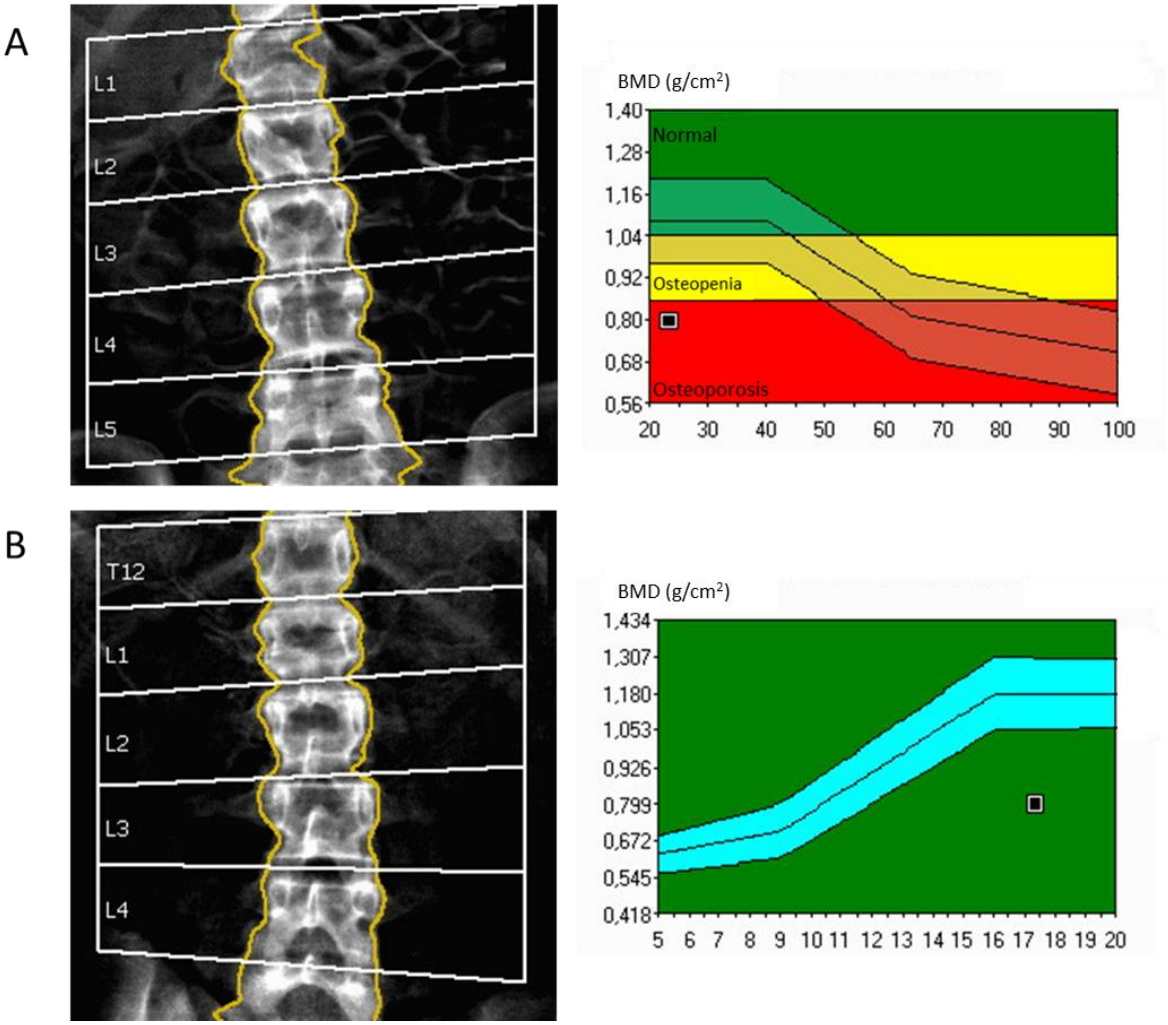

Figure S5 : Osteodensitometry analysis showing low bone densities of the two patients of Family B

(A) Patient B.II.3 at 23 years old and (B) Patient B.II.4 at 17 years old.

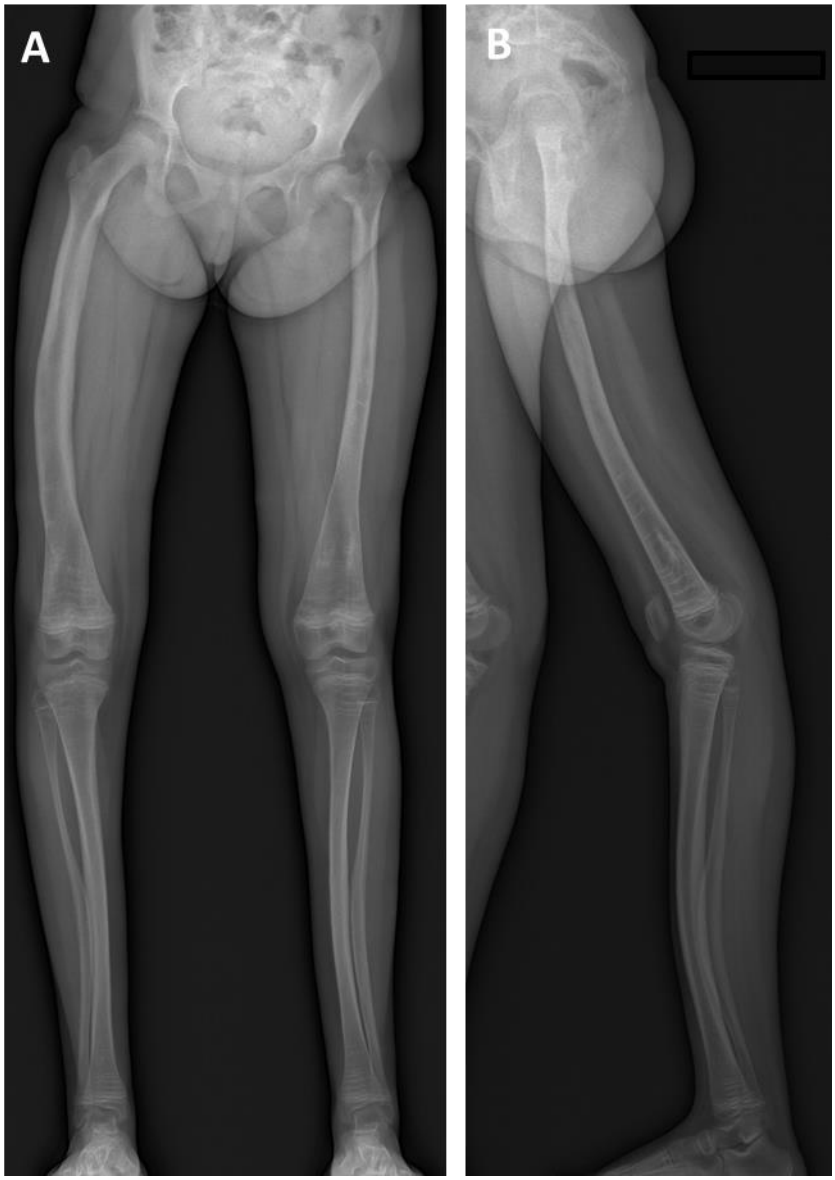

Figure S6 : Lower limb X-ray of Patient B.II.4 at 15 years old showing abnormalities of the bone remodeling with femoral deformation, bone demineralization and Left Coxa vara.

(A) front view. (B) lateral view.

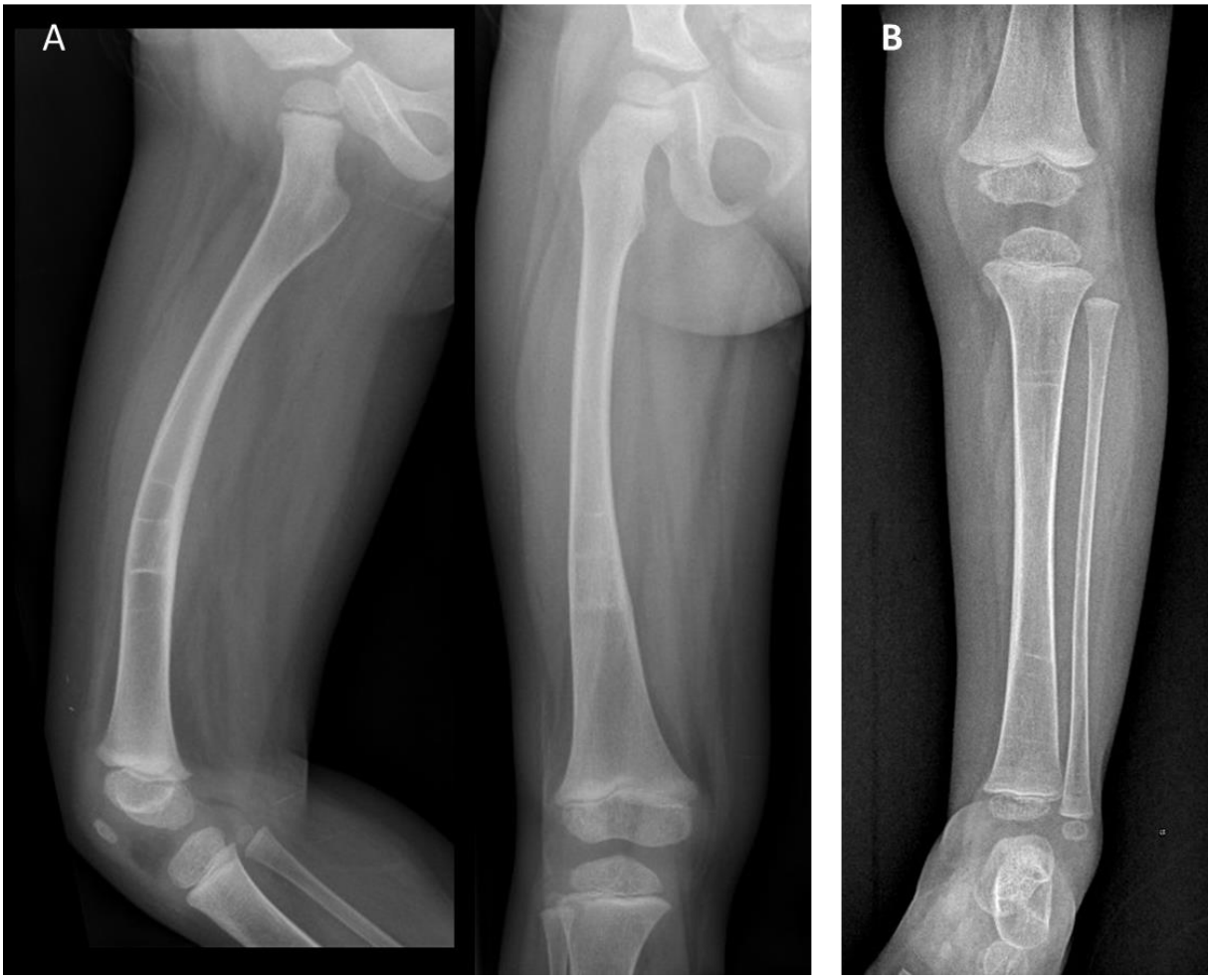

Figure S7: X-ray of Patient C.II.1 femur (A) and tibia (B) showing bone demineralization (2 years old)

```
tr|A0A0R4IU52|A0A0R4IU52_DANRE      MSQDSSALREEGNNHFKAGDVQQALTCYTKALKISDCPSESAVLYRNRSACYLKLEDYTK
tr|F1QU23|F1QU23_DANRE              MSQDSSALREEGNNHFKAGDVQQALTCYTKALKISDCPSESAVLYRNRSACYLKLEDYTK
tr|Q567I0|Q567I0_DANRE             MSQDSSALREEGNNHFKAGDVQQALTCYTKALKISDCPSESAVLYRNRSACYLKLEDYTK
                                    ************************************************************

tr|A0A0R4IU52|A0A0R4IU52_DANRE      AEEDATKSLDVDPGDIKARFRRAQALQKLGRLDQAFMDVQKCAQLEPKNKAFQDLLRQLG
tr|F1QU23|F1QU23_DANRE              AEEDATKSLDVDPGDIKARFRRAQALQKLGRLDQAFMDVQKCAQLEPKNKAFQDLLRQLG
tr|Q567I0|Q567I0_DANRE             AEEDATKSLDVDPGDIKARFRRAQALQKLGRLDQAFMDVQKCAQLEPKNKAFQDLLRQLG
                                    ************************************************************

tr|A0A0R4IU52|A0A0R4IU52_DANRE      AQIQQKATQLSSTDSRVQQMFKLLLDSSAPIADRQKAAQNLVVLSREDAGAEQIFRNDGV
tr|F1QU23|F1QU23_DANRE              AQIQQKATQLSSTDSRVQQMFKLLLDSSAPIADRQKAAQNLVVLSREDAGAEQIFRNDGV
tr|Q567I0|Q567I0_DANRE             AQIQQKATQLSSTDSRVQQMFKLLLDSSAPIADRQKAAQNLVVLSREDAGAEQIFRNDGV
                                    ************************************************************

tr|A0A0R4IU52|A0A0R4IU52_DANRE      KLLQNLLESKQEELILSALRTLVGLCTGHQSRDRVWTPLDYDYSTVMCKY----------
tr|F1QU23|F1QU23_DANRE              KLLQNLLESKQEELILSALRTLVGLCTGHQSRTMAIVNE-L-GMERLCGVMGSSASSVSL
tr|Q567I0|Q567I0_DANRE             KLLQNLLESKQEELILSALRTLVGLCTGHQSRTEFGHP----------------------
                                    ********************************

tr|A0A0R4IU52|A0A0R4IU52_DANRE      ------------------------------------------------------------
tr|F1QU23|F1QU23_DANRE              SACHLLQVMFEALTEGMKKRIRGKDEAILPEPSRELRSMLRHLLDMLPASSVSGAGRDSA
tr|Q567I0|Q567I0_DANRE             ------------------------------------------------------------

tr|A0A0R4IU52|A0A0R4IU52_DANRE      ------------------------------------------------------------
tr|F1QU23|F1QU23_DANRE              INLLVKQVPRKSVKNPDNSLSLWVIDQGLKKILEVAGTVAEVENGPPLTENTHMSCSVLL
tr|Q567I0|Q567I0_DANRE             ------------------------------------------------------------

tr|A0A0R4IU52|A0A0R4IU52_DANRE      ------------------------------------------------------------
tr|F1QU23|F1QU23_DANRE              NKLYDDLKSDKERENFSKLCEEYVQHHFMSSSMERRLRAIQTVSVLLQGPSDVGNVTLEL
tr|Q567I0|Q567I0_DANRE             ------------------------------------------------------------

tr|A0A0R4IU52|A0A0R4IU52_DANRE      ------------------------------------------------------------
tr|F1QU23|F1QU23_DANRE              SGLMDSVISLCASEDIVQQQVAVEALIHAAGKAKRASFITANGVALLKELYKKSQNDRIR
tr|Q567I0|Q567I0_DANRE             ------------------------------------------------------------

tr|A0A0R4IU52|A0A0R4IU52_DANRE      ------------------------------------------------------------
tr|F1QU23|F1QU23_DANRE              VRALVGLCKLGSAGGTDFSMKQFAEGSTLKLAKQCRKWLCNESLPPASRRWAIEGLAYLT
tr|Q567I0|Q567I0_DANRE             ------------------------------------------------------------

tr|A0A0R4IU52|A0A0R4IU52_DANRE      ------------------------------------------------------------
tr|F1QU23|F1QU23_DANRE              LDADVKEDLVEDKKALQAMFELAKSEDKTVLFAVGSTLVNCTNSYDVEKPDPQMVELAKY
tr|Q567I0|Q567I0_DANRE             ------------------------------------------------------------

tr|A0A0R4IU52|A0A0R4IU52_DANRE      ------------------------------------------------------------
tr|F1QU23|F1QU23_DANRE              AKQHVPEEHPKDGQPFVEQRVVKLLEAGVVSALVCMVKQESPAMTEACRECIARVILALV
tr|Q567I0|Q567I0_DANRE             ------------------------------------------------------------

tr|A0A0R4IU52|A0A0R4IU52_DANRE      ------------------------------------------------------------
tr|F1QU23|F1QU23_DANRE              ERQEDRGLVVAQGGGKALLPLVSESTDRGKIKAAQALAKITITSNPEIAFPGERVYEVVR
tr|Q567I0|Q567I0_DANRE             ------------------------------------------------------------

tr|A0A0R4IU52|A0A0R4IU52_DANRE      ------------------------------------------------------------
tr|F1QU23|F1QU23_DANRE              PLVSLLALDCSMLQNFEALMALTNLAGISERLRQKIIKEKAVPKIEGYMFEEHDMVRAAS
tr|Q567I0|Q567I0_DANRE             ------------------------------------------------------------

tr|A0A0R4IU52|A0A0R4IU52_DANRE      ------------------------------------------------------------
tr|F1QU23|F1QU23_DANRE              TECMCNLALSTEVQKLYLAAESDRLKLLVLYSGEDDERLRKAASGTLAVLTGEMPELCTR
tr|Q567I0|Q567I0_DANRE             ------------------------------------------------------------

tr|A0A0R4IU52|A0A0R4IU52_DANRE      ------------------------------------------------------------
tr|F1QU23|F1QU23_DANRE              IPDTTSHWLEILQALLLSESQDLRHRGVVIVMNIMQADKSLAEKLMESEALEILSVLTKT
tr|Q567I0|Q567I0_DANRE             ------------------------------------------------------------

tr|A0A0R4IU52|A0A0R4IU52_DANRE      ------------------------------------
tr|F1QU23|F1QU23_DANRE              DDPKQASVRKAAQRCLDLALEYGLIRSNESGVNGNSI
```

Figure S8: Protein sequence alignment of the 3 UNC45A isoforms from Danio Rerio :

ENSDART00000159409.2 (F1QU23), ENSDART00000171709.1 (A0A0R4IU52) and ENSDART00000163426.1 (Q567I0) CLUSTAL O(1.2.4) multiple sequence alignment.

Figure S9 : Protein sequence alignment of UNC45A (Q9H3U1.1) from homo sapiens and UNC45A from Danio Rerio (F1QU23) with CLUSTAL O(1.2.4) multiple sequence alignment

The mutations found in the Family A, B and C are indicated in blue, red and green respectively

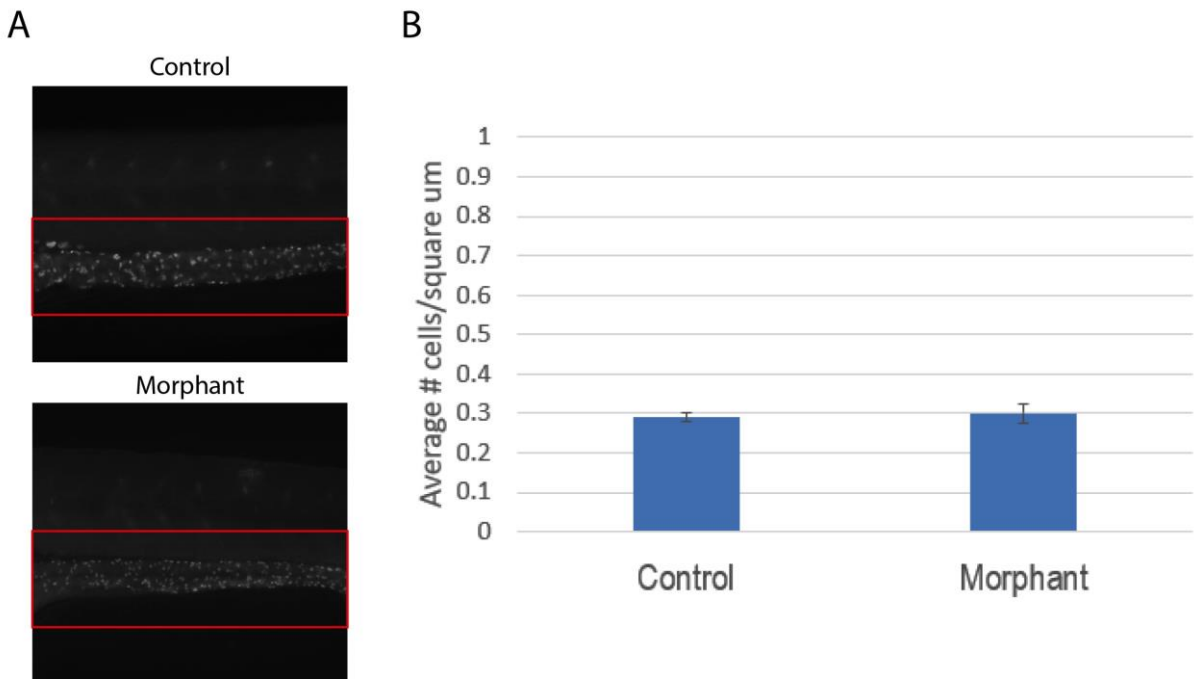

Figure S10: Enteric neuron analysis suggests that unc45a suppression does not impact neurodevelopment in the gut.

A. Antibody staining against HuC/D in whole mount zebrafish and B. the quantified the region of the number of neurons/square um in the gut (T-test p-value=0.418). Supplementary

Supplemental table

Individual	Exon	Mutation	gnomeAD frequency	UMD Predictor (score)	Polyphen (score)	SIFT
A.II.2	11	c.784C>T:p.Arg262*	3/277220	Pathogenic (100)		
	14	c.1268T>A:p.Val423Asp	NS	Pathogenic (99)	Probably damaging (0.996)	Affected Protein Function
B.II.3 ; B.II.4	23	c.2581C>T:pGln861*	NS	Pathogenic (100)		
	23	c.2633C>T:p.Ser878Leu	7/277162	Pathogenic (99)	Probably damaging (0.996)	Affected Protein Function
	23	c.2734T>G:p.Cys912Gly	NS			
C.II.1	8	c.247C>T:p.Arg83Trp	4/276948	Pathogenic (100)	Probably damaging (1)	Affected Protein Function
	13	c.983G>T:p.Gly328Val	NS	Pathogenic (100)	Probably damaging (1)	Affected Protein Function

Table S1 : *UNC45A* mutations and pathogenicity prediction

Mutations in *UNC45A*, gnomAD (genome Aggregation Database) frequency and prediction of the pathogenicity. (NS stand for Never Seen)

Supplemental References

1. Altschul, S.F., Madden, T.L., Schaffer, A.A., Zhang, J., Zhang, Z., Miller, W., and Lipman, D.J. (1997). Gapped BLAST and PSI-BLAST: a new generation of protein database search programs. Nucleic acids research 25, 3389-3402.

2. Katoh, K., and Standley, D.M. (2013). MAFFT multiple sequence alignment software version 7: improvements in performance and usability. Molecular biology and evolution 30, 772-780.
3. Criscuolo, A., and Gribaldo, S. (2010). BMGE (Block Mapping and Gathering with Entropy): a new software for selection of phylogenetic informative regions from multiple sequence alignments. BMC evolutionary biology 10, 210.
4. Nguyen, L.T., Schmidt, H.A., von Haeseler, A., and Minh, B.Q. (2015). IQ-TREE: a fast and effective stochastic algorithm for estimating maximum-likelihood phylogenies. Molecular biology and evolution 32, 268-274.
5. Ronquist, F., Teslenko, M., van der Mark, P., Ayres, D.L., Darling, A., Hohna, S., Larget, B., Liu, L., Suchard, M.A., and Huelsenbeck, J.P. (2012). MrBayes 3.2: efficient Bayesian phylogenetic inference and model choice across a large model space. Systematic biology 61, 539-542.